

Chemical composition of a sample of candidate post-AGB stars

S. Sumangala Rao^{1*}, Sunetra Giridhar¹ and David L. Lambert²

¹Indian Institute of Astrophysics, Bangalore 560034, India

²W. J. McDonald Observatory, The University of Texas, Austin, Texas, USA 78712

26 October 2018

ABSTRACT

We have derived elemental abundances for a sample of nine IRAS sources with colours similar to those of post-AGB stars. For IRAS 01259+6823, IRAS 05208-2035, IRAS 04535+3747 and IRAS 08187-1905 this is the first detailed abundance analysis based upon high resolution spectra. Mild indication of s-processing for IRAS 01259+6823, IRAS 05208-2035 and IRAS 08187-1905 have been found and a more comprehensive study of s-process enhanced objects IRAS 17279-1119 and IRAS 22223+4327 have been carried out.

We have also made a contemporary abundance analysis of the high galactic latitude supergiants BD+39° 4926 and HD 107369. The former is heavily depleted in refractories and estimated [Zn/H] of -0.7 dex most likely gives initial metallicity of the star. For HD 107369 the abundances of α and Fe-peak elements are similar to those of halo objects and moderate deficiency of s-process elements is seen. IRAS 07140-2321 despite being a short period binary with circumstellar shell does not exhibit selective depletion of refractory elements.

We have compiled the stellar parameters and abundances for post-AGB stars with s-process enhancement, those showing significant depletion of condensable elements and those showing neither. The compilation shows that the s-process enhanced group contains very small number of binaries, and observed $[\alpha/\text{Fe}]$ are generally similar to thick disc values. It is likely that they represent AGB evolution of single stars.

The compilation of depleted group contains larger fraction of binaries and generally supports the hypothesis of dusty discs surrounding binary post-AGB stars inferred via the shape of their SED and mid IR interferometry. IRAS 07140-2321 and BD+39° 4926 are difficult to explain with this scenario and indicate the existence of additional parameter/condition needed to explain the depletion phenomenon. However the conditions for discernible depletion, minimum temperature of 5000K and initial metallicity larger than -1.0 dex found from our earlier work still serves as useful criteria.

Subject headings: stars:abundances – stars:AGB and post-AGB – stars: variables:other (RV Tauri)

Key words: Post-AGB stars, abundances, circumstellar matter: stars.

1 INTRODUCTION

Considerable theoretical and observational interest has in recent years been focused on asymptotic giant branch (AGB) stars but much remains mysterious about them. The AGB phase is enjoyed by low and intermediate mass stars (approximate mass range 0.8 to $8M_{\odot}$). It is in this phase that a star experiences extensive internal nucleosynthesis whose

fruits are dredged to the stellar surface (see Herwig 2005). Furthermore, mass-loss ensures that the products of nucleosynthesis are dispersed into the circumstellar and subsequently the interstellar environment. Thus, AGB stars are likely major contributors of Li, C, N, F and s-process elements among others to Galactic chemical evolution (Romano et al. 2010).

Observational validation of theoretical investigations of how AGB stars achieve internal nucleosynthesis, dredge-up and mass-loss are generally hampered by the fact that the more evolved and more interesting of these stars have low

* E-mail: sumangala@iiap.res.in (SR); giridhar@iiap.res.in (SG); dll@astro.as.utexas.edu (DLL)

temperature atmospheres and therefore spectra replete with dense and complex molecular lines. Although these spectra have been analysed by a few stellar spectroscopists, the abundance studies are generally limited to very few elements and isotopic ratios.

The AGB phase of stellar evolution concludes with a rapid phase of evolution to the tip of the white dwarf cooling track. This post-AGB (PAGB) phase takes a star in a few thousand years or so from a cool AGB star to a very hot central star of a planetary nebula and onto a white dwarf cooling track. Along this track, the star's spectrum is amenable to straightforward abundance analysis and thus offers apparently a way to infer the abundance changes brought by the PAGB star's AGB progenitor. This inference is, of course, dependent on the assumption that the composition of an AGB star is exactly preserved by the PAGB star. Observations of certain PAGB stars show that this is a false assumption. For example, several PAGB stars show abundance anomalies correlated with the condensation temperature (T_C)¹ for dust grains to condense out of gas of normal composition (see Van Winckel 2003 for a review) – a process we refer to as ‘dust-gas winnowing’. Other PAGB candidate stars show abundance anomalies correlated with the ionization potential of the neutral atoms (Rao & Reddy 2005) – a process we refer to as ‘the FIP effect’.

Given that the PAGB phase is rapid, the number of identified PAGB stars is relatively small and the number subjected to an abundance analysis is, of course, even smaller. In this paper, we report abundance analyses for 11 candidate PAGB stars and have compiled abundance data of previously analysed PAGB stars in an attempt to seek explanations for the diverse compositions of these objects.

2 SELECTION OF THE SAMPLE

Our sample stars are presented in Table 1 and displayed in the IRAS two colour diagram Figure 1 which has proven to be a powerful tool for identifying candidate PAGB stars (van der Veen & Habing 1988; Suárez et al. 2006; Szczerba et al. 2007). Nine of our eleven stars have measured IRAS fluxes and are identified in Figure 1; the stars, HD 107369 and BD +39° 4926 were not detected by IRAS.

It is known that zone 1 of IRAS two colour diagram by van der Veen & Habing 1988 corresponds to fluxes from stellar photospheres warmer than 2000K. The IRAS colours of Zones II-III signify the emergence and evolution of circumstellar shell (CS) produced by increasing large mass-loss at AGB. Sources at Zone IV are at the super-wind phases or slightly beyond. Zone V contains objects with only signature of cold dust shell as the mass-loss has stopped hence warm dust is not being added. The objects with detached cold CS would be seen at region VIa, while objects in zone VIb contains objects with warm as well as cold CS. The

¹ The condensation temperature T_C is the temperature at which half of a particular element in a gaseous environment condenses into dust grains. Condensable elements refer to the refractories like Ti, Ca, Sc and the s-process elements which readily condense into dust grains because of their high T_C .

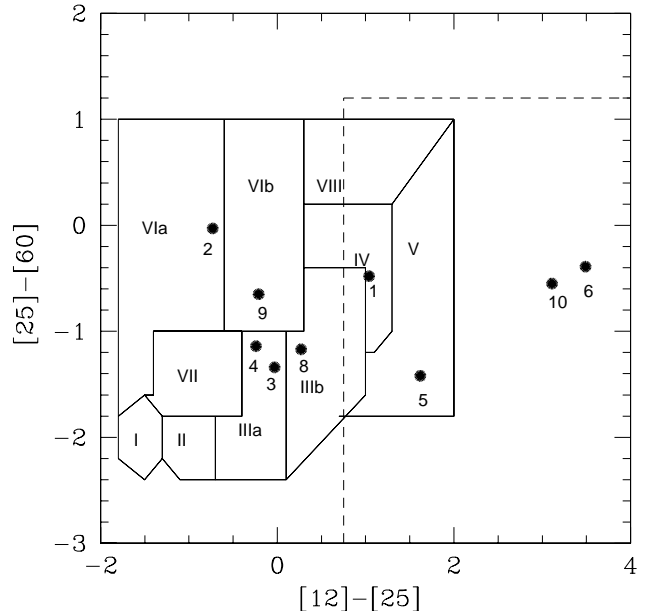


Figure 1. The location of sample stars in IRAS color-color diagram containing the zones defined by van der Veen & Habing (1988) and area enclosed in the dashed line which according to Szczerba et al. 2007 is richly populated by PAGB stars with colours like planetary nebulae. The sample stars are numbered as follows: 1- IRAS 01259+6823 2- IRAS 04535+3747 3- IRAS 05208-2035 4- IRAS 07140-2321 5- IRAS 07331+0021 6- IRAS 08187-1905 8- IRAS 12538-2611 9- IRAS 17279-1119 10- IRAS 22223+4327

Zone VII and dashed region is dominated by PAGBs with PN like colours.

Our sample stars IRAS 05208-2035, IRAS 07140-2321, IRAS 12538-2611 and IRAS 01259+6823 belong to zone IIIa, IIIb and IV where signatures of CS formed by increased mass-loss at late AGB are evident. IRAS 17279-1119 (zone VIb) seems to possess the hot as well as cold dust shell while IRAS 07331+0021, IRAS 22223+4327, IRAS 08187-1905 have PN like colours.

3 OBSERVATIONS

High-resolution optical spectra were obtained at the W.J. McDonald Observatory with the 2.7m Harlan J. Smith reflector and the Tull coude spectrograph (Tull et al. 1995) with a resolving power of 60,000. Spectral coverage in a single exposure from this cross-dispersed echelle spectrograph is complete up to 6000\AA and extensive but incomplete at longer wavelengths. A S/N ratio of 80-100 over much of the spectral range was achieved. Figure 2 contains a few representative spectra to illustrate the quality of typical spectra.

Table 1. The Program Stars.

No.	IRAS	Other Names	Var Type	Colors
1	01259+6823	PN like
2	04535+3747	V409 Aur, HD 280138, BD+37°996	SRD	...
3	05208-2035	BD-20°1073	...	RV Tauri like
4	07140-2321	CD-23°5180, SAO 173329	Irregular	RV Tauri like
5	07331+0021	AI CMi, BD+00° 2006	Irregular	...
6	08187-1905	V552 Pup, HD 70379, BD-18° 2290	SRD	...
7	...	HD107369, SAO 203367
8	12538-2611	HR 4912, HD 112374, BD-18° 2290	SRD	RV Tauri like
9	17279-1119	HD 158616, BD-11°4391, V340 Ser	RV Tauri	RV Tauri like
10	22223+4327	V448 Lac, BD +42° 4388	SRD	PN like
11	...	BD+39°4926, SAO 72704

Table 2. Stellar Parameters Derived from the Fe-line Analyses

Star	UT Date	V_r^a (km s ⁻¹)	$T_{\text{eff}}, \log g, [\text{Fe}/\text{H}]$	ξ_t^b (km s ⁻¹)	Fe I ^c		Fe II ^c	
					log ϵ	n	log ϵ	n
IRAS01259+6823	2007 Nov 5	-49.1	5000, 1.50, -0.60	3.3	6.82 ± 0.10	60	6.88 ± 0.11	11
IRAS04535+3747	2008 Feb 29	-37.4	6000, 1.25, -0.48	3.6	6.96 ± 0.19	97	6.99 ± 0.10	12
IRAS05208-2035	2007 Nov 3	+50.3	4250, 0.75, -0.65	1.6	6.80 ± 0.20	49	6.81 ± 0.11	7
IRAS07140-2321	2007 Nov 2	+68.0	7000, 1.00, -0.92	3.6	6.55 ± 0.14	75	6.52 ± 0.11	19
IRAS07331+0021	2008 Apr 19	+47.9	4500, 1.00, -1.16	5.2	6.27 ± 0.16	26	6.32 ± 0.10	4
IRAS08187-1905	2008 Feb 26	+ 61.5	6250, 0.50, -0.59	3.8	6.90 ± 0.15	33	6.82 ± 0.13	11
HD107369	2008 Apr 20	-39.0	7500, 1.50, -1.33	1.3	6.09 ± 0.13	19	6.15 ± 0.12	30
IRAS12538-2611	2009 May 10	-31.3	5250, 1.00, -1.12	4.6	6.34 ± 0.11	59	6.33 ± 0.11	12
IRAS17279-1119	2008 Aug 10	+68.7	7250, 2.25, -0.43	4.7	7.02 ± 0.21	21	7.01 ± 0.16	12
IRAS22223+4327	2009 Dec 27	-41.3	6500, 1.00, -0.33	4.3	7.14 ± 0.08	20	7.11 ± 0.10	16
BD +39° 4926	2007 Nov 19	-36.3	7750, 1.00, -2.37	3.0	5.02 ± 0.15	9	5.15 ± 0.13	21

^a V_r is the radial velocity in km s⁻¹

^b ξ_t is the microturbulence

^clog ϵ is the mean abundance relative to H (with log $\epsilon_H = 12.00$). The standard deviations of the means as calculated from the line-to-line scatter are given. n is the number of considered lines.

4 ABUNDANCE ANALYSIS

We have made use of the new grid of ATLAS09 model atmospheres available at database of Kurucz². Spectrum synthesis code MOOG (2009 version) by C. Sneden (1973) has been used. The assumptions are standard, Local Thermodynamical Equilibrium (LTE), plane parallel atmosphere and hydrostatic equilibrium and flux conservation.

The hydrogen lines for most stars were affected by emission components hence could not be used for parametrization of stars. We have used Fe I and Fe II lines for deriving atmospheric parameters. Further, lines of Mg I, Mg II; Si I, Si II; Ti I, Ti II and Cr I, Cr II were also used as additional constraints whenever possible.

Our sample stars were generally hotter than 5000K with the exception of IRAS 07331+0021 and IRAS 05208-2035, which fortunately turned out to be metal-poor by -1.2 dex and -0.65 dex. Hence adequate number of unsaturated clean lines could be measured for number of elements for them.

First, the microturbulence ξ_t is derived by requiring that the derived abundances are independent of line strengths. We have generally used Fe II lines for measuring ξ_t

microturbulence for most of our sample stars, since appreciable departure from LTE are known to occur for Fe I lines (Boyarchuk et al. 1985, Thévenin & Idiart 1999). However for coolest members, IRAS 05208-2035 and IRAS 07331+0021 very few Fe II lines could be measured and hence Fe I lines had to be used instead for fixing the microturbulence.

The temperature is estimated by requiring that derived abundances are independent of the Lower Excitation Potential (LEP). IRAS 07140-2321, HD 107369 and BD+39°4926 had large number of useable Fe II lines. In fact, for HD 107369 Fe II lines cover good LEP range to estimate the temperature. For IRAS 07140-2321 and BD+39°4926 the LEP covered by Fe II lines was lesser than those by Fe I hence both species were employed although we did not find any difference between the temperatures estimated from them. For cool stars the observed Fe II did not have a good range in LEP hence Fe I lines were employed. The gravity was derived by requiring Fe I and Fe II giving the same abundance. In addition, the ionization equilibrium of Mg I/ Mg II, Si I/Si II, Sc I/Sc II, Ti I/Ti II, Cr I/Cr II were used as additional constraints whenever possible.

The accuracy of equivalent width measurements depends on resolution, spectral type of the star and the continuum fitting. For stars of spectral type late A- F, the equiv-

² <http://kurucz.harvard.edu/grids.html>

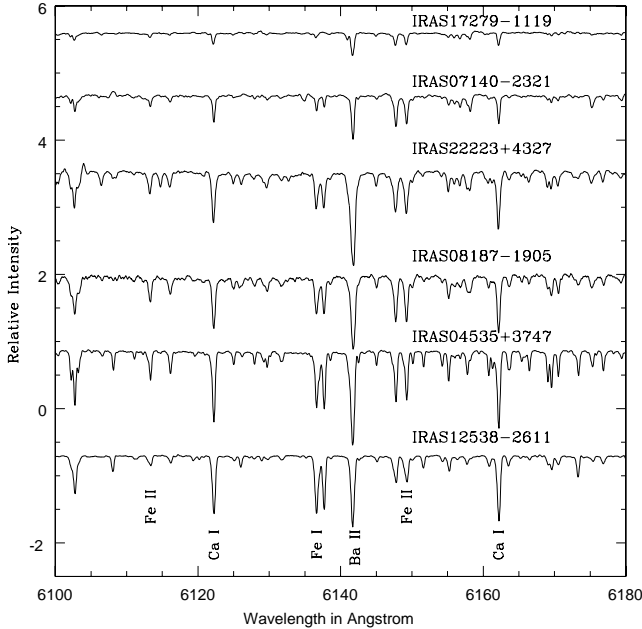


Figure 2. Sample spectra of our stars presented in descending order of temperature (top to bottom) in the 6100-6180 region.

alent widths could be measured with an accuracy of $\sim 5-8\%$ in absence of line asymmetries.

With the above mentioned accuracy in measured equivalent widths, the microturbulence velocity could be measured with an accuracy of $\pm 0.25 \text{ km s}^{-1}$, temperature with $\pm 150\text{K}$ and $\log g$ of $\pm 0.25 \text{ cm s}^{-2}$.

But for cooler stars, line strengths could only be measured with accuracy of 8-10%. The microturbulence velocity could be measured with an accuracy of $\pm 0.5 \text{ km s}^{-1}$, temperature with $\pm 250\text{K}$ and $\log g$ of $\pm 0.5 \text{ cm s}^{-2}$.

The derived atmospheric parameters and heliocentric radial velocities for the epoch of observations for the program stars are presented in Table 2.

The sensitivity of the derived abundances to the uncertainties of atmospheric parameters T_{eff} , $\log g$, and ξ are summarized in Table 3. For four stars representing the full temperature range of our sample, we present changes in $[X/\text{Fe}]$ caused by varying atmospheric parameters by 200K, 0.25 cm s^{-2} and 0.5 km s^{-1} (average accuracies of these parameters) with respect to the chosen model for each star.

The total stellar parameter related error is estimated by taking the square root of the sum of the square of the systematic errors (individual errors associated with uncertainties in temperatures and gravities) and bars in the abundance plot correspond to the systematic error.

Having determined the atmospheric parameters, the abundances of different elements were derived using the available lines. The derived abundances relative to the solar abundances are presented in their respective tables. The solar photospheric abundances given by Asplund, Grevesse & Sauval (2005) have been used as reference values.

The sources of the gf values for different elements used in our abundance analysis have been listed in Table 4.

We have investigated possible systematic effects caused

by the adopted gf values from different sources as follows. We have measured solar equivalent widths for our lines on Solar Flux Atlas by Kurucz et al. (1984) and estimated the abundances using model atmosphere appropriate for the sun $T_{\text{eff}}=5770$, $\log g$ of 4.4 and ξ_t of 0.9 km s^{-1} . The agreement for most elements is within 0.04 to 0.09 dex although the linelist is different for different stars.

The lines of certain elements are affected by hyperfine splitting. We have included the hyperfine structure components in our line list while synthesizing the spectral feature of these elements for deriving the abundances. For elements Sc and Mn, we have used hfs component list and their $\log gf$ given by Prochaska & McWilliam (2000), for Cu (Allen & Porto de Mello 2011), for Eu (Mucciarelli et al. 2008) and for Ba (McWilliam 1998). The effect of isotopic components were considered for Eu II (2 isotopes) and Ba II (5 isotopes) lines.

4.1 The errors caused by assumption of LTE

Non-LTE corrections for CNO elements show strong temperature dependence (particularly for N see e.g. Lyubimkov et al. 2011, Schiller & Przybilla 2008) and they also vary from multiplet to multiplet. Venn (1995) have tabulated these corrections for C and N for a range of stellar temperatures for lines belonging to different multiplets. For B-F stars the correction for N varies from -0.3 dex to -1.0 dex while for C it is -0.1 to -0.5 dex. Takeda and Takada-Hidai (1998) have calculated Non-LTE corrections for oxygen abundance using 6156-6158Å lines for A-F stars and correction varies between -0.1 to -0.4 dex.

The neglect of departure from LTE also introduces errors in the estimated abundances of heavier elements. These errors for a given element vary with the stellar temperatures and also on metallicities. In very metal-poor stars the over-ionisation and in some cases usage of resonance lines for abundance determination results in errors as large as $+0.5$ dex for elements like Na. We have only used subordinates lines for sodium, believed to be formed in deeper layers and for them Non-LTE corrections of about -0.10 dex are reported (Lind et al. 2011, Gehren et al. 2004). Gehren et al have estimated Non-LTE corrections for Mg and Al and for the lines used in our analysis for a sample of G stars covering a range in metallicities. For thick disc metallicities Non-LTE corrections are $+0.05$ for $[\text{Mg}/\text{Fe}]$ and $+0.2$ for $[\text{Al}/\text{Fe}]$ is reported. The Non-LTE corrections for S I lines have been estimated by Korotin (2009). For the S I lines used in our work (6042 – 6056, 6743 – 6758 Å), the effect is negligible. Wedemeyer (2001) has done Non-LTE calculation for Si I lines and Non-LTE correction in range -0.01 to -0.05 have been estimated for the Sun and Vega respectively. Mashonkina, Korn and Przybilla (2007) have studied departure from LTE over a range of stellar parameter and metallicities for a large number of Ca I and Ca II lines. At solar or moderately deficient metallicities the Non-LTE correction is smaller than $+0.1$ dex for Ca I lines used in our analysis for deriving Ca abundance. Also the correction is negligible for very weak Ca I features. Bergemann(2011) have computed Non-LTE Ti I and Ti II for late type stars. At solar temperatures the Non-LTE corrections between $+0.05$ to 0.10 dex are found for Ti I lines while the effect is negligible for Ti II lines. Bergemann suggests the use of only Ti II

Table 3. Sensitivity of $[X/Fe]$ to the uncertainties in the model parameters for a range of temperatures covering our sample stars .

Species	IRAS 05208-2035 (4250K)			IRAS 12538-2611 (5250K)			IRAS 22223+4327 (6500K)			BD +39°4926 (7750K)		
	ΔT_{eff} -200K	$\Delta \log g$ +0.25	$\Delta \xi$ +0.5	ΔT_{eff} -200K	$\Delta \log g$ +0.25	$\Delta \xi$ +0.5	ΔT_{eff} -200K	$\Delta \log g$ +0.25	$\Delta \xi$ +0.5	ΔT_{eff} -200K	$\Delta \log g$ +0.25	$\Delta \xi$ +0.5
C I	-0.31	-0.07	-0.02	+0.10	+0.01	-0.03	-0.03	+0.06	+0.06
N I	+0.19	-0.04	-0.02	-0.27	-0.09	+0.04
O I	+0.30	-0.03	-0.13	+0.03	-0.06	-0.03	+0.22	-0.05	-0.03	-0.24	-0.08	+0.01
Na I	+0.21	+0.09	-0.01	+0.04	+0.07	-0.03	-0.03	+0.10	-0.03	+0.02	+0.13	+0.01
Mg I	+0.18	+0.09	+0.06	+0.06	+0.06	-0.03	-0.08	+0.10	+0.06	+0.09	+0.12	+0.00
Al I	+0.22	+0.07	-0.09	+0.02	+0.07	-0.05	-0.04	+0.12	-0.05	+0.07	+0.13	-0.01
Si I	-0.03	+0.02	-0.10	+0.01	+0.06	-0.04	-0.03	+0.10	-0.03
Si II	+0.17	-0.07	+0.09	-0.32	-0.11	+0.01
S I	-0.23	-0.02	-0.04	+0.03	+0.05	-0.03	+0.00	+0.10	-0.01
Ca I	+0.24	+0.08	+0.03	+0.07	+0.06	-0.02	-0.07	+0.11	+0.01
Ca II	+0.13	-0.04	-0.04
Sc II	-0.44	-0.06	-0.01	-0.01	-0.09	-0.02	-0.01	-0.08	-0.01
Ti I	+0.35	+0.06	+0.00	+0.28	-0.07	+0.01
Ti II	+0.14	-0.01	+0.01	-0.06	-0.19	+0.05	+0.00	-0.10	+0.07	-0.04	-0.10	+0.00
Cr I	+0.25	+0.07	+0.36	+0.20	+0.08	-0.02
Cr II	-0.08	+0.00	-0.04	-0.16	+0.03	-0.01	+0.06	-0.08	+0.00	-0.08	-0.10	+0.00
Mn I	+0.19	+0.03	-0.01	-0.07	+0.09	-0.02
Co I	+0.00	+0.00	+0.10
Ni I	+0.13	+0.02	+0.11	+0.13	+0.06	-0.04	-0.07	+0.10	-0.03
Cu I	+0.15	+0.06	-0.04
Zn I	+0.06	+0.02	+0.02	-0.07	+0.10	-0.02	+0.06	+0.12	-0.01
Y II	+0.18	-0.01	+0.00	-0.04	-0.04	-0.01	-0.02	-0.09	+0.01
Zr I	+0.43	+0.01	+0.03
Zr II	+0.00	-0.08	+0.01
Mo I	+0.40	+0.04	-0.09
Ba II	+0.04	-0.08	+0.04
La II	+0.29	-0.02	-0.08	-0.05	-0.05	-0.02
Ce II	+0.24	-0.02	-0.12	-0.06	-0.06	+0.01
Pr II	+0.31	-0.02	-0.11	-0.18	-0.02	-0.04
Nd II	+0.26	-0.02	-0.08	-0.12	-0.03	-0.01
Sm II	+0.29	-0.01	-0.02	-0.03	-0.05	-0.02

lines and $[Ti/Fe]$ computed from Ti II and Fe II would be more robust. Non-LTE analysis of Cr I and Cr II by Bergemann & Cescutti (2010) for solar and metal-poor stars indicate an error of -0.1 dex at the solar metallicities which becomes larger $+0.3$ to 0.5 dex for very metal-poor stars. Non-LTE effects for Fe I and Fe II lines have been estimated by Mashonkina (2011) for A-F stars with more complete representation of model atom. It is found that LTE underestimates the abundance derived from Fe I lines by 0.02 to 0.1 dex depending upon the chosen line and stellar temperatures; the effect could be as large as 0.2 dex for giants. The Non-LTE corrections are very small for Fe II lines. While deriving gravities from ionisation equilibrium of Fe I & Fe II, relatively large Non-LTE corrections for Fe I must be taken into consideration. Velichko, Mashonkina & Nilsson (2010) have calculated Non-LTE correction for Zr I and Zr II lines; both species become weak in LTE. The Non-LTE correction for Zr II lines used and for our stellar parameters range does not exceed $+0.1$ dex. Our sample stars are F-K supergiants with metallicity range 0 to -1.2 . To disentangle the evolutionary effects (on abundances) from those inherent to the natal ISM we have compared the observed abundance pattern with those characterized for thin and thick disc by extensive studies like Bensby et al. 2005, Reddy et al. 2006 using extended samples of F-G dwarfs and subgiants and

more recently by Takeda, Sato and Murata (2008) using late G giants. Between these samples the $[X/Fe]$ vs $[Fe/H]$ plots are remarkably similar for elements Si, Ca, Sc, Ti, V, Cr, Mn, Co, Ni and Cu and Non-LTE effects for these elements are also generally very small. Hence it is possible to infer the population type of the sample stars from important abundance ratios such as $[\alpha/Fe]$ given for various disc components from the above mentioned studies. As explained above, the Non-LTE effects for α elements are not large enough to mask the characteristic abundance differences.

5 RESULTS

Results of our abundance analyses are presented in this section. If the candidate PAGB star has preserved the composition of its AGB progenitor, the C, N, O (and Li) abundances betray information about the abundance changes brought by the first and second dredge-ups in the giant prior to the AGB and changes brought about by the third dredge-up on the AGB. **We also look for the signature of Hot Bottom Burning (HBB) which can operate if the star had a massive progenitor ($M > 4M_{\odot}$) (Ventura & D'Antona 2009) and its manifestation can produce enrichments of Li, N, Na, Mg and Al (Blöcker**

& Schönberner 1991). Abundances of elements from Si through the iron group are expected to be unchanged as a star evolves from the main sequence to the AGB phase. These abundances may, in principle, be used to assign a stellar population to the star, e.g., thin disc, thick disc or halo. Beyond the iron group, abundances of *s*-process nuclides are predicted to be enriched in AGB stars that experienced the third dredge-up. Such nuclides dominate elements such as Y, Zr and Ba.

If the PAGB star has been subject to dust-gas winnowing or to selective diffusion of elements according to the first ionization potential (the FIP effect), abundance anomalies will be present that are unrelated to those arising from nucleosynthesis.

In this section, we present an abundance analysis for each star and comment briefly on the abundance anomalies, if any. The primary initial goal is to draw attention to the observational clues, if any, to the prior action of the third dredge-up on the AGB and, thus, to the C, N, and O abundances as well as the indicators of *s*-process contamination. Another goal is to scan the anomalies for dust-gas winnowing and/or the FIP effect.

We postpone to Section 5.13 a discussion of abundances, especially the $[X/Fe]$ values, which might betray the stellar population from which the PAGB is drawn. One potential indicator of population is the abundance of α elements Mg, Si, S, Ca and Ti which have a higher ratio in thick disc stars than in the thin disc at the same $[Fe/H]$. This postponement arises in large part from the fact that in essentially every star the $[\alpha/Fe]$ ratios do not consistently point to a thick or a thin disc origin. The α -elements are sending a mixed message whose interpretation is best discussed for the whole sample.

5.1 IRAS 01259+6823

Our analysis appears to be the first detailed abundance analysis for this star with our final abundances presented in Table 5. A low resolution spectrum presented by Suárez et al. (2006) shows an absorption spectrum with emission limited to $H\alpha$. Stellar lines are sharp (FWHM about 0.26\AA corresponding to 14 km s^{-1}) and symmetric at our resolution.

Atmospheric parameters (Table 2) estimated from Fe I and Fe II lines were found to give satisfactory ionization equilibrium for Si, Ti, Cr and Fe: $\Delta = [X_{II}/H] - [X_I/H]$ is $+0.21, -0.03, +0.22$ and $+0.06$ for Si, Ti, Cr and Fe respectively. The question of thick vs thin disc is discussed for the sample as whole in Section 5.13.

Of the elements anticipated to be affected by internal nucleosynthesis and dredge-up by the termination of the AGB phase, C with $[C/Fe] = +0.2$ appears enriched slightly by the third dredge-up in a AGB star; C is lowered by the first dredge-up with $[C/Fe] \simeq -0.2$. The C/O ratio of 0.4 by number shows that the star is not carbon-rich and, hence, the third dredge-up was mild. A mild *s*-process enrichment is seen according to Y, Zr and Ba, with $[s/Fe] \simeq +0.3$ with a slightly higher enrichment for the so-called heavy *s* elements (e.g., Ba) than for the light *s* elements (e.g., Y and Zr). Inspection of the abundances shows no sign for operation of dust-gas winnowing or the FIP effect. In short, IRAS 01259+6823 evolved at an early phase off the AGB before dredge-up from the He-shell began in earnest.

5.2 IRAS 04535+3747

This is the first abundance analysis for this SRD variable which with an effective temperature of 6000K has presumably evolved from the AGB or possibly the horizontal branch. **The star occupies the box VIa in the IRAS two colour diagram (Figure 1). This position is occupied by objects having detached cold CS dust shells.**

Strong absorption lines have a weak asymmetry in their blue wings. This asymmetry has been ignored in the measurement of the equivalent width. We assume that a classical atmosphere may be used for the abundance analysis. Model atmosphere parameters are given in Table 2 and the final abundances have been presented in Table 5.

The star is mildly metal-poor ($[Fe/H] = -0.48$). Ionization equilibrium is adequately achieved not only for Fe but also for Si, Ti and Cr: $\Delta = [X_{II}/H] - [X_I/H]$ is $-0.04, -0.14, +0.01$ and $+0.03$ for Si, Ti, Cr and Fe respectively.

This star has not evolved from an AGB star in which the third dredge-up has enriched the atmosphere in C and the *s*-process. The C/O ratio of 0.3 by number is that expected of a star at the beginning of the AGB and the *s*-process has not enriched the heavy elements. To within the uncertainties about the initial C, N and O abundances, their alterations by the first dredge-up and the errors of the abundance analysis, the C, N and O abundances are those anticipated for a star beginning the AGB **following either a stay on the horizontal branch or may execute blue loops given the present uncertainties in the masses of SRD's.**

5.3 IRAS 05208-2035

The infrared excess is typical of RV Tauri variables (De Ruyter et al. 2006). De Ruyter et al. complain lack of a published spectrum and of estimates for the stellar parameters. This lack we correct here. An orbital period of 236 days has been reported in Gielen et al. (2008).

The chosen model (Table 2) gives the abundances as presented in Table 6. Ionization equilibrium is satisfactorily accounted for in that $\Delta = [X_{II}/H] - [X_I/H]$ is $+0.01, -0.02,$ and $+0.05$ for Fe, Ti and Cr respectively. In terms of the evolutionary history, the most significant aspect of the star's composition is an enhancement of the heavy elements. In particular, those elements (e.g., Y, Zr and Ba) dominated by an *s*-process contribution are overabundant relative to Fe by about 0.3 dex. The *r*-process dominated elements (e.g., Eu) are also overabundant but this is as expected for a star of $[Fe/H] = -0.6$. Although the star is a spectroscopic binary and thus a candidate for dust-gas winnowing, this effect is absent but this is not surprising given the extensive convective envelope of such a cool star.

5.4 IRAS 07140-2321

IRAS 07140-2321 (also known as SAO 173329) is a PAGB star belonging to a spectroscopic binary with a dusty circumbinary disc (Van Winckel et al. 2000, De Ruyter et al. 2006; Gielen et al. 2008). The orbital period is 116 days (De Ruyter et al. 2006). Photometrically, the star is an irregular small amplitude variable for which Kiss et al. (2007) suggests variations with periods of about 24 and 60 days. Here,

Table 4. References for the log *gf* values

Species	Accuracy ^a	Ref	Species	Accuracy ^a	Ref
C	B-C	1	Fe II	A-B	9
N	B-C	1	Co	B-C	10
O	B-C	2	Ni	B-D	10
Na	A	3	Cu	B-D	11
Mg	B-C	4	Zn	B-D	11
Al	B-D	5	Y	B-D	12
Si	B-D	6	Zr	B-D	13
S	D	22	Ba	B-D	21
Ca	C-D	23	La	B-D	14
Sc	D	7	Ce	B-D	15
Ti	B-D	7	Pr	B-D	16
V	B-D	7	Nd	B-D	17
Cr	B-C	20	Sm	B-D	18
Mn	B-C	7	Eu	B-D	19
Fe I	A-B	8	Dy	B-D	16

^aSymbols indicating the accuracy of the *gf* values where A = $\pm 3\%$, B = $\pm 10\%$, C = $\pm 25\%$ and D = $\pm 50\%$

¹Wiese et al. 2007, ²Wiese et al. 1996, ³Sansonetti (2008), ⁴Kelleher et al. 2008a

⁵Kelleher et al. 2008b, ⁶Kelleher et al. 2008c, ⁷Martin et al. 1988, ⁸Fuhr et al. 2006

⁹Meléndez & Barbuy (2009), ¹⁰Fuhr et al. 1988, ¹¹Fuhr et al. 2005, ¹²Hannaford et al. 1982

¹³Biémont et al. 1981, ¹⁴Lawler et al. 2001a, ¹⁵Lawler et al. 2009

¹⁶Snedden et al. 2009, ¹⁷Den Hartog et al. 2003, ¹⁸Lawler et al. 2006, ¹⁹Lawler et al. 2001b,

²⁰Sobeck et al. 2007, ²¹Curry (2004), ²²Podobedova et al. 2009, ²³Aldenius et al. 2009

we are responding to a call by Van Winckel (1997) who published the only previously reported abundance analysis and wrote ‘SAO 173329 is a metal-deficient object for which more data are needed’. Specifically, Van Winckel noted the lack of an oxygen abundance determination and the need for ‘more good Fe II lines’. The lack of abundance data for heavy or *s*-process elements was also a notable omission.

Results from our analysis summarized in Table 6 are based on the model atmosphere summarized in Table 2. The star is metal-poor: $[\text{Fe}/\text{H}] = -0.9$. The C/O ratio of 0.4 and the limited data on heavy element abundances show that this star did not evolve from a thermally pulsing AGB star. The N abundance shows evidence of N enrichment by the First Dredge-Up (FDU). The observed $[\text{N}/\text{Fe}]$ after Non-LTE correction of -0.4 dex (Lyubimkov et al. 2011) is $+0.3$ dex which is similar to FDU prediction of $+0.5$ dex as given in Schaller (1992). Heavy elements – Y, Zr and Ba are not enriched relative to Fe. For elements in common, our abundances are in fair agreement with those reported by Van Winckel (1997) who used solar *gf*-values and a different grid of model atmospheres. Abundance differences between those in Table 6 and those reported by Van Winckel for a 7000 K model atmosphere are small (except for Si I and Cr I): δ $[\text{X}/\text{Fe}]$ (present work – VW97) is -0.20 dex for C I, $+0.11$ dex for N I, $+0.43$ dex for Si I, -0.22 for Ca I, -0.22 for Ti II, -0.37 for Cr I, $+0.14$ for Mn I, $+0.13$ for Ni I and -0.03 for Zn I.

The inspection of the estimated abundances shows that the observed $[\text{S}/\text{Fe}]$ is $+0.6$; the possible α enrichment of $+0.3$ dex expected at $[\text{Fe}/\text{H}]$ of -0.9 may indicate actual $[\text{S}/\text{Fe}]$ of $+0.3$ dex. But nearly zero $[\text{Zn}/\text{Fe}]$ and lack of depletion for high T_C elements Ca and Sc shows that the star

is not affected by dust-gas winnowing. It is surprising given the fact that the star is a spectroscopic binary with an orbital period of only 115.9 days (Van Winckel & Reyniers 2000) and has detected circumstellar material. It appears that conditions for effective dust-gas winnowing are far from understood.

5.5 IRAS 07331+0021

This cool variable exhibits TiO bands in its spectrum at its coolest phases (Klochkova & Panchuk 1996) which necessarily impair a full abundance analysis at such phases. Luck & Bond (1989) undertook an analysis of an image-tube spectrum obtained in 1981 and found the star was metal-poor ($[\text{Fe}/\text{H}] = -1.0$) with a larger under-abundance of *s*-process elements. Noting that all of the elements deficient with respect to iron had second ionization potentials less than the ionization potential of hydrogen, they speculated that Lyman continuum emission from shock waves in the atmosphere over-ionized these elements and therefore they appear under-abundant when a standard analysis with a classical atmosphere is performed. Klochkova & Panchuk (1996, 1998) reported abundance analyses from CCD spectra of AI CMi taken at three different epochs. Results for the separate phases are given in their 1996 paper and average results with the addition of O and Zn are provided in the 1998 paper. Inspection of the 1996 tabulation of abundances shows that results for several species vary from spectrum to spectrum: for example, the $[\text{Sc}/\text{Fe}]$ ratio is variously given as -0.63 , -0.22 , and -0.05 . Luck & Bond’s shocking hypothesis might allow for this kind of variation. From their comparison with Luck & Bond’s results, Klochkova & Panchuk

Table 5. Elemental Abundances for IRAS 01259+6823 and IRAS 04535+3747.

Species	$\log \epsilon_{\odot}$	IRAS 01259+6823			IRAS 04535+3747		
		[X/H]	N	[X/Fe]	[X/H]	N	[X/Fe]
C I	8.39	-0.42 ± 0.08	2	+0.18	-0.43 ± 0.10	5	+0.05
N I	7.78	...			$+0.24 \pm 0.08$	5	+0.72
O I	8.66	-0.29 ± 0.08	2	+0.31	-0.17 ± 0.11	3	+0.31
Na I	6.17	-0.25 ± 0.05	3	+0.35	$+0.05 \pm 0.04$	3	+0.53
Mg I	7.53	-0.52 ± 0.10	2	+0.08	-0.46 ± 0.14	4	+0.02
Al I	6.37	-0.68 ± 0.14	3	-0.08	-0.42 ± 0.19	3	+0.06
Si I	7.51	-0.40 ± 0.09	10	+0.20	-0.27 ± 0.14	16	+0.21
Si II	7.51	-0.19 ± 0.03	2	+0.41	-0.31 ± 0.17	2	+0.17
S I	7.14	-0.43	synth	+0.17	-0.16 ± 0.15	2	+0.32
Ca I	6.31	-0.79 ± 0.09	11	-0.19	-0.59 ± 0.19	13	-0.11
Sc II	3.05	-0.80 ± 0.02	synth	-0.20	-0.75 ± 0.00	synth	-0.27
Ti I	4.90	-0.67 ± 0.11	11	-0.07	-0.56 ± 0.13	13	-0.08
Ti II	4.90	-0.70 ± 0.08	3	-0.10	-0.70 ± 0.08	5	-0.22
V I	4.00	-0.80 ± 0.11	11	-0.20	...		
Cr I	5.64	-0.74 ± 0.07	4	-0.14	-0.58 ± 0.12	8	-0.10
Cr II	5.64	-0.52 ± 0.04	4	+0.08	-0.57 ± 0.09	5	-0.09
Mn I	5.39	-0.72 ± 0.08	7	-0.12	-0.62 ± 0.14	7	-0.14
Fe	7.45	-0.60			-0.48		
Co I	4.91	-0.75 ± 0.11	3	-0.15	...		
Ni I	6.23	-0.79 ± 0.15	21	-0.19	-0.53 ± 0.14	23	-0.05
Zn I	4.60	-0.69 ± 0.10	3	-0.09	-0.53 ± 0.13	3	-0.05
Sr I	2.92	-0.30 ± 0.00	1	+0.30	...		
Y II	2.21	-0.53 ± 0.11	5	+0.07	-0.40 ± 0.20	13	+0.08
Zr II	2.58	-0.48 ± 0.02	2	+0.12	-0.49 ± 0.17	5	-0.01
Ba II	2.17	-0.04 ± 0.00	synth	+0.56	...		
La II	1.13	-0.19 ± 0.10	3	+0.41	-0.33 ± 0.23	2	+0.15
Ce II	1.58	-0.36 ± 0.05	8	+0.24	-0.42 ± 0.13	18	+0.06
Pr II	0.78	-0.48 ± 0.06	3	+0.12	-0.31 ± 0.23	3	+0.17
Nd II	1.46	-0.38 ± 0.07	10	+0.22	-0.42 ± 0.08	5	+0.06
Sm II	0.95	-0.30 ± 0.10	5	+0.30	-0.44 ± 0.05	3	+0.04
Eu II	0.52	-0.31 ± 0.01	synth	+0.29	...		
Dy II	1.14	...			-0.65 ± 0.00	2	-0.17

(1996) conclude that the two analyses are in good agreement. They further write 'We come to the conclusion that from 1981 to 1995 abundances of elements heavier than oxygen remained the same in the AI CMi atmosphere, i.e., no transfers of matter processed in the inner layers of the star to the star's atmosphere is observed.'

Our spectrum taken on April 19, 2008 exhibits strong bands of CN, CH, MgH and TiO. Strong lines exhibit blue-shifted components. The atmospheric parameters (Table 2) fall within the range reported by Klochkova and Panchuk (1998). We estimate [Fe/H] of -1.16 while KP1998 derive -1.14 . For the most elements the abundances derived by us agree with KP1998. Our analysis covers additional elements C, Co and Sm (see Table 6). Of note is that our analysis and that of KP1998 do not confirm the under-abundance of heavy elements reported by Luck & Bond. Heavy elements have a normal abundance for a star with [Fe/H] = -1.16 . The C and especially the O abundance are unusually high. C abundance has been measured from 5380.3 and O from [O I] lines. A fair conclusion may be that the star like others in our sample has not experienced the full effect of the third dredge-up on the AGB branch.

5.6 IRAS 08187-1905

High-resolution optical spectra have not been previously reported. Low resolution spectroscopy and photometry was obtained by (Reddy & Parthasarathy 1996). Our abundance analysis (Table 7) with the model atmosphere in Table 2 suggests that the star is slightly metal-poor ([Fe/H] = -0.6) and is C-rich. The O abundance is as expected for a [Fe/H] = -0.6 star but the C enrichment suggests addition of C to the original material. Formally, C/O by number of atoms slightly exceeds unity. The light-*s* elements Y and Zr as well as the heavy *s* element Ba point to a mild *s*-process enrichment. One is led to suggest that the star, after a FDU which decreased the C and increased the N abundance, experienced the third dredge-up which increased the C abundance and thus the C/O ratio and also mildly enriched the *s*-process content of the atmosphere.

5.7 HD 107369

This high-galactic latitude F supergiant is not an IRAS source. Van Winckel (1997) who undertook an abundance analysis using high-resolution spectra of selected wavelength intervals found the star to be metal-poor ([Fe/H] = -1.3). Our abundance analysis with the model in Table 2 is re-

Table 6. Elemental Abundances for IRAS 05208-2035, IRAS 07140-2321 and IRAS 07331+0021

Species	IRAS 05208-2035			IRAS 07140-2321			IRAS 07331+0021			
	$\log \epsilon_{\odot}$	[X/H]	N	[X/Fe]	[X/H]	N	[X/Fe]	[X/H]	N	[X/Fe]
C I	8.39			-0.61 ± 0.10	12	+0.31	-0.44 ± 0.03	2	+0.72
N I	7.78			-0.15 ± 0.16	4	+0.77	...		
O I	8.66	-0.25 ± 0.27	2	+0.40	-0.54 ± 0.00	1	+0.38	$+0.04 \pm 0.09$	2	+1.20
Na I	6.17	-0.22 ± 0.09	5	+0.43	-0.40 ± 0.16	4	+0.52	...		
Mg I	7.53	-0.52 ± 0.14	2	+0.13	-0.61 ± 0.14	3	+0.31	-0.68 ± 0.00	1	+0.48
Mg II	7.53	...			-0.74 ± 0.00	1	+0.18	...		
Al I	6.37	-0.45 ± 0.05	4	+0.20	-1.18 ± 0.00	1	-0.26		
Si I	7.51	-0.56 ± 0.19	8	+0.09	-0.56 ± 0.12	5	+0.36	-0.89 ± 0.24	5	+0.27
Si II	7.51	...			-0.74 ± 0.00	1	+0.18	...		
S I	7.14	...			-0.32 ± 0.04	3	+0.60	...		
Ca I	6.31	-0.79 ± 0.13	6	-0.14	-0.97 ± 0.19	15	-0.05	-1.25 ± 0.09	3	-0.09
Sc II	3.05	...			-0.92 ± 0.13	9	+0.00	-1.35 ± 0.15	2	-0.19
Ti I	4.90	-0.52 ± 0.24	15	+0.13		
Ti II	4.90	-0.54 ± 0.26	4	+0.11	-0.73 ± 0.14	8	+0.19	-0.89 ± 0.05	5	+0.27
Cr I	5.64	-0.64 ± 0.12	6	+0.01	-0.71 ± 0.10	4	+0.21	-0.98 ± 0.16	2	+0.18
Cr II	5.64	-0.59 ± 0.00	2	+0.06	-0.74 ± 0.05	5	+0.18	-0.97 ± 0.10	2	+0.19
Mn I	5.39	...			-1.00 ± 0.01	synth	-0.08	-1.35 ± 0.08	3	-0.19
Fe	7.45	-0.65			-0.92			-1.16		
Co I	4.92	-0.53 ± 0.08	2	+0.12			-0.97 ± 0.11	6	+0.19
Ni I	6.23	-0.44 ± 0.17	13	+0.21	-0.85 ± 0.07	7	+0.07	-1.19 ± 0.10	10	-0.03
Cu I	4.21			-1.30 ± 0.08	synth	-0.14
Zn I	4.60	...			-0.87 ± 0.16	2	+0.05	...		
Y II	2.21	-0.41 ± 0.16	4	+0.24	-1.10 ± 0.13	5	-0.18	-1.15 ± 0.00	1	+0.01
Zr I	2.59	-0.30 ± 0.10	4	+0.35		
Mo I	1.92	-0.16 ± 0.12	2	+0.49		
Ba II	2.17	-0.34 ± 0.00	synth	+0.31	-0.64 ± 0.00	synth	+0.28	...		
La II	1.13	-0.31 ± 0.15	3	+0.34	...			-0.89 ± 0.11	3	+0.27
Ce II	1.58	-0.29 ± 0.05	2	+0.36	...			-1.22 ± 0.00	1	-0.06
Pr II	0.71	-0.40 ± 0.00	1	+0.25	...			-1.02 ± 0.00	1	+0.14
Nd II	1.45	-0.31 ± 0.11	6	+0.34	...			-1.36 ± 0.22	2	-0.20
Sm II	1.01	-0.39 ± 0.18	3	+0.26	...			-1.02 ± 0.13	5	+0.14
Eu II	0.52	-0.51 ± 0.03	synth	+0.14		

ported in Table 7. We estimate a temperature of 7500K and $\log g$ of 1.5 using the Fe I and Fe II lines. However, the estimated gravity is also supported by ionization equilibrium of Mg I & Mg II, Ca I & Ca II, Cr I & Cr II. Our abundances are in good agreement with Van Winckel's results. To make comparison easy we have used his line strengths with new set of gf values and models. The scanty Fe line data supports the temperature and gravity estimated by us. Adopting our model (7500,1.5,2.2) we find following δ (present work - VW1997) +0.34 dex for N I, +0.13 dex for O I, +0.18 for Si II, +0.24 for S I, -0.09 for Ca I, +0.26 for Ti II, -0.03 for Cr II, +0.06 for Fe I, +0.12 for Fe II and +0.04 for Ba II respectively. Our analysis covers additional elements Mg, Ni, Sr and Y. The star does not provide the expected abundance signature of a typical AGB star such as C/O greater than one and a strong s -process enrichment. Nor do we see any indication of dust-gas winnowing. The lines of Zn were not detectable.

The elements with higher condensation temperature such as Ca, Sc did not exhibit expected depletion. The N abundance appears very high at $[N/Fe] = +1.15$ and in excess of the value expected by the FDU. However, Non-LTE corrections for the N I lines are -0.5 dex from Lyubimkov et al. 2011 is indicated. After applying this correction we get $[N/Fe]$ of +0.7 dex which is marginally larger than predic-

tion of FDU. Van Winckel reported $[C/Fe]$ of -0.2 dex from a single line. There is no compelling evidence for HBB in the form of very large $[N/Fe]$ nor do we see Li I feature. **Being a high galactic latitude metal-poor object it does not seem to have evolved from a massive progenitor since $M > 4M_{\odot}$ is required for HBB (Ventura & D'Antona 2009).** With low C/O ratio, high galactic latitude and low metallicity it appears to have evolved from a low mass progenitor.

5.8 IRAS 12538-2611

Also known as HR 4912, this variable star was studied spectroscopically by Luck, Lambert and Bond (1983) (LLB83) who found it metal-poor ($[Fe/H] = -1.2$). With its high luminosity it is quite likely to be a PAGB object. An abundance analysis was also performed by Giridhar, Arellano Ferro and Parrao (1997) (GAFP97). Our spectra have better resolution and spectral coverage than earlier studies. There is fair agreement between our abundances and those by LLB83 and GAFP97. The run of C, N and O abundances offer no evidence that the star evolved from a thermally pulsing AGB star: the C/O ratio is 0.06 by number of atoms (see Table 7). The N abundance (estimated by LLB83) before correction

Table 7. Elemental Abundances for IRAS 08187-1905, HD 107369 and IRAS 12538-2611

Species	IRAS 08187-1905				HD 107369			IRAS 12538-2611		
	$\log \epsilon_{\odot}$	[X/H]	N	[X/Fe]	[X/H]	N	[X/Fe]	[X/H]	N	[X/Fe]
C I	8.39	+0.03 ± 0.25	9	+0.62	...			-1.09 ± 0.13	3	+0.03
N I	7.78	-0.10 ± 0.23	4	+0.49	-0.18 ± 0.25	5	+1.15	...		
O I	8.66	-0.33 ± 0.24	3	+0.26	-0.68 ± 0.09	4	+0.65	-0.17 ± 0.01	2	+0.95
Na I	6.17	+0.03 ± 0.19	3	+0.62	...			-0.61 ± 0.05	3	+0.51
Mg I	7.53	-0.46 ± 0.19	3	+0.13	-0.95 ± 0.04	2	+0.38	-0.80 ± 0.00	1	+0.32
Mg II	7.53	...			-0.77 ± 0.04	2	+0.56	...		
Al I	6.37			-1.38 ± 0.11	2	-0.26
Si I	7.51	-0.11 ± 0.15	5	+0.48	...			-0.89 ± 0.19	6	+0.23
Si II	7.51	...			-0.80 ± 0.24	4	+0.53	...		
S I	7.14	+0.05 ± 0.06	3	+0.64	-0.84	synth	+0.49	-0.69 ± 0.01	2	+0.43
Ca I	6.31	-0.63 ± 0.17	8	-0.05	-1.28 ± 0.09	3	+0.05	-1.34 ± 0.14	10	-0.22
Ca II	6.31			-1.43 ± 0.00	1	-0.10	...		
Sc II	3.05	-0.75 ± 0.00	synth	-0.16	-1.45	synth	-0.12	-1.55 ± 0.03	synth	-0.43
Ti I	4.90			-0.81 ± 0.00	1	+0.31
Ti II	4.90	-0.99 ± 0.10	2	-0.40	-1.09 ± 0.10	18	+0.24	-0.89 ± 0.19	6	+0.23
Cr I	5.64	-0.52 ± 0.15	3	+0.07	-1.52 ± 0.05	2	-0.19	-1.50 ± 0.02	2	-0.38
Cr II	5.64	-0.66 ± 0.14	7	-0.08	-1.43 ± 0.10	7	-0.10	-1.49 ± 0.05	4	-0.37
Mn I	5.39			-1.52 ± 0.06	2	-0.40
Fe	7.45	-0.59			-1.33			-1.12		
Ni I	6.23	-0.60 ± 0.11	7	-0.01	-1.05 ± 0.04	2	+0.28	-1.13 ± 0.18	11	-0.01
Zn I	4.60	-0.58 ± 0.16	3	+0.01	...			-1.04 ± 0.06	2	+0.08
Sr II	2.92	...			-1.85 ± 0.00	1	-0.52	...		
Y II	2.21	-0.19 ± 0.20	4	+0.40	-1.81 ± 0.07	2	-0.48	-1.28 ± 0.09	2	-0.16
Zr II	2.59	-0.33 ± 0.14	2	+0.25		
Ba II	2.17	-0.34 ± 0.00	synth	+0.25	-1.80 ± 0.12	2	-0.47	-1.34 ± 0.00	1	-0.22
La II	1.13			-1.37 ± 0.05	2	-0.25
Ce II	1.58			-1.45 ± 0.07	3	-0.33
Nd II	1.45			-1.51 ± 0.07	3	-0.39

for Non-LTE effects is consistent with that expected from the FDU. There is no evidence for *s*-process enrichment.

5.9 IRAS 17279-1119

This PAGB star has been the subject of two previous abundance analyses. In introducing IRAS 17279-1119, Van Winckel (1997) hereinafter VW97 noted that optical photometry shows that it has some RV Tauri-like characteristics with possible periods of 61 and 93 days (Bogaert 1994) but additional photometry is needed; inspection of SIMBAD shows that photometry has not been reported recently. Van Winckel's abundance analysis for a model atmosphere with $T_{\text{eff}} = 7400\text{K}$ and $\log g = 0.5$ showed the star to be metal-poor ($[\text{Fe}/\text{H}] = -0.7$) with a C/O close to unity and possibly exceeding unity and *s*-process enriched, both markers of prior third dredge-up on the AGB. His discussion of the star concluded with the observation that "this as yet poorly studied star deserves further research". An appreciated limitation of Van Winckel's analysis was the limited wavelength coverage of his spectroscopic snapshots. Arellano Ferro, Giridhar & Mathias (2001) hereinafter AGM2001 acquired new spectra with complete coverage from 3900-6800 Å which enabled them to determine the abundances of all elements considered by VW97 (except for N) and add Na, Mg, Mn, La and Ce to the list. The star was again shown to be metal-poor ($[\text{Fe}/\text{H}] = -0.6$) and *s*-process enriched. Unusual aspects of the composition are found from these analyses. Most striking

perhaps, AGM2001 found $[\text{Na}/\text{Fe}] = +0.6$ and from both analyses a high Sc abundance was reported, $[\text{Sc}/\text{Fe}] = +0.9$ (VW97 from one Sc II line) and +0.6 (AGM2001 from eight Sc II lines).

Since the solar abundances used by AGM2001 and VW97 are different from our work we have transformed these abundances to the abundance scale of Asplund et al. (2005) for comparison. The present analysis covers additional elements Sr, Zr, Pr and Nd (see Table 8). In general, the results of the present analysis agree well with those of prior analyses. An exception is that we do not confirm the anomalously high Sc abundance reported by VW97 and AGM2001.

The progenitor of IRAS 17279-1119 was likely a thermally pulsing AGB star. This suggestion accounts for the C/O of unity and the modest *s*-process enrichment.

5.10 IRAS 22223+4327

This star has been classified as a proto-planetary nebula and, therefore, a PAGB star (Hrivnak 1995, Kwok 1993). Even on a low resolution spectrum, Hrivnak (1995) could see the enhancement of lines of *s*-process elements. From the UVB photometry, Arhipova et al. (2003) found this star to be pulsating variable with a period of ~ 90 days.

Long term monitoring of this star using high resolution spectra has been carried out by Klochkova, Panchuck & Tavalzhanskaya (2010) with following interesting findings. The strong absorption lines such as low excitation line of

Table 8. Elemental Abundances for IRAS 17279-1119, IRAS 22223+4327 and BD +39 4926

Species	log ϵ_{\odot}	IRAS 17279-1119			IRAS 22223+4327			BD +39 4926		
		[X/H]	N	[X/Fe]	[X/H]	N	[X/Fe]	[X/H]	N	[X/Fe]
C I	8.39	-0.08 ± 0.17	11	+0.35	$+0.27 \pm 0.14$	20	+0.60	$+0.05 \pm 0.12$	17	+2.42
N I	7.78	$+0.20 \pm 0.12$	4	+0.63	$+0.33 \pm 0.01$	2	+0.66	$+0.52 \pm 0.26$	9	+2.89
O I	8.66	-0.31 ± 0.00	1	+0.12	$+0.07 \pm 0.05$	2	+0.40	$+0.19 \pm 0.09$	10	+2.56
Na I	6.17	-0.04 ± 0.12	2	+0.39	$+0.10 \pm 0.06$	2	+0.43	-0.39 ± 0.17	2	+1.98
Mg I	7.53	-0.42 ± 0.10	3	+0.01	$+0.07 \pm 0.09$	2	+0.40	-1.91 ± 0.15	4	+0.46
Al I	6.37	...			$+0.15 \pm 0.01$	2	+0.48	-2.79 ± 0.00	1	-0.42
Si I	7.51	-0.19 ± 0.22	4	+0.24	$+0.09 \pm 0.07$	4	+0.42	..		
Si II	7.51	-0.24 ± 0.09	2	+0.19	$+0.06 \pm 0.00$	1	+0.39	-1.87 ± 0.25	6	+0.50
S I	7.14	$+0.03 \pm 0.12$	4	+0.46	$+0.25 \pm 0.10$	2	+0.58	$+0.07 \pm 0.17$	4	+2.44
Ca I	6.31	-0.54 ± 0.19	7	-0.11	-0.20 ± 0.09	8	+0.13	..		
Ca II	6.31	...			-0.22 ± 0.08	2	+0.11	...		
Sc II	3.05	-0.43 ± 0.03	synth	+0.00	-0.38 ± 0.05	2	-0.05	-2.80 ± 0.08	2	-0.43
Ti II	4.90	$+0.04 \pm 0.22$	6	+0.47	-0.17 ± 0.08	6	+0.16	-2.73 ± 0.14	10	-0.36
Cr II	5.64	-0.53 ± 0.02	3	-0.09	-0.41 ± 0.15	8	-0.08	-2.07 ± 0.15	5	+0.30
Mn I	5.39	-0.62 ± 0.27	2	-0.19	-0.46 ± 0.05	2	-0.13	...		
Fe	7.45	-0.43			-0.33			-2.37		
Ni I	6.23	-0.60 ± 0.43	2	-0.17	-0.22 ± 0.11	11	+0.11	...		
Zn I	4.60	-0.28 ± 0.11	2	+0.15	-0.45 ± 0.00	1	-0.12	-0.70 ± 0.08	2	+1.67
Sr I	2.92	-0.20 ± 0.00	1	+0.23		
Y II	2.21	$+0.50 \pm 0.22$	5	+0.93	$+1.15 \pm 0.15$	3	+1.48	...		
Zr II	2.58	$+0.52 \pm 0.07$	2	+0.95	$+0.82 \pm 0.16$	5	+1.15	..		
Ba II	2.17	$+0.16 \pm 0.00$	synth	+0.59	$+1.16 \pm 0.00$	synth	+1.49	..		
La II	1.13	$+0.18 \pm 0.17$	2	+0.61	$+0.97 \pm 0.14$	16	+1.30	...		
Ce II	1.58	$+0.43 \pm 0.11$	7	+0.86	$+0.48 \pm 0.13$	11	+0.81	..		
Pr II	0.78	$+0.00 \pm 0.00$	1	+0.43	$+0.70 \pm 0.09$	5	+1.03	..		
Nd II	1.45	$+0.26 \pm 0.06$	2	+0.69	$+0.60 \pm 0.10$	14	+0.93	..		
Sm II	0.95	...			$+0.50 \pm 0.07$	5	+0.83	...		
Eu II	0.52	...			$+0.10 \pm 0.01$	synth	+0.43	...		

Ba II at 6141 Å not only show asymmetries in the profile with short wavelength side of the profile showing extended wing than the red wing; these strong lines also show large amplitude profile variations (with time) caused by variations in blue wing while red wing remained unchanged. The spectrum contains C₂ lines most likely formed in the circumstellar shell. At the epoch of largest asymmetry in strong Ba II line the C₂ (0;1) band head at λ 5635 is seen in emission. The cores of hydrogen lines show larger variations in radial velocities (~ 8 kms⁻¹) while weak metallic lines show smaller amplitude variations in radial velocities (~ 1 kms⁻¹). Molecular C₂ lines remain stationary with time; the shift in circumstellar features relative to systemic velocity gives an expansion velocity V_{exp} of 15.0 kms⁻¹. Our spectrum taken on Dec 27, 2009 also exhibits the features mentioned in Klochkova, Panchuck & Tavalzhanskaya (2010). This star was analysed by Van Winckel and Reyniers (2000) (hereinafter WR2000) who found it moderately metal-poor [Fe/H] of -0.3 dex and showing enhancement of s-process elements. The present analysis covers additional elements Na, Mg and Zn and uses larger number of lines for many species (see Table 8). Since the solar abundances used in WR2000 are different from our work, we have transformed these abundances to solar abundances of Asplund et al. (2005) to facilitate comparison. All elements agree within ± 0.15 dex.

IRAS 22223+4327's progenitor was most probably a thermally pulsing AGB star. This is indicated by the C/O ratio of unity and the about one dex enrichment of the s-process elements. Two of our program stars IRAS 17279-

1119 and IRAS 22223+4327 show significant s-process enhancement. We have compared the spectra of these two objects with IRAS 07140-2321 with similar temperature but without s-process enhancement in **Figure 3**.

5.11 BD+39°4926

Although this object has been mentioned in several papers on PAGB stars, a contemporary abundance analysis using high-quality digital spectra, modern model atmospheres and refined atomic data has not been undertaken. Abundance data from Kodaira et al. (1970) show strong effects of dust-gas winnowing. Yet, this star unlike other stars exhibiting severe dust-gas winnowing does not have an infrared excess. However, the star is a spectroscopic binary, as are many or even all other stars exhibiting severe dust-gas winnowing. For these reasons, we chose to include this object in our sample.

Our spectral coverage (particularly in red region) has been more extensive and we could make a more detailed analysis employing more number of lines per species and also including the important element Zn. The star's final abundances are presented in Table 8. Figure 4 shows the plot of [X/H] vs [T_C] for this star. This star shows a clear indication of the dust-gas separation without possessing IR indications of circumstellar envelope. From this plot, we infer that the initial metallicity of the star is -0.7 dex. (Another such star showing selective depletion of refractory elements without

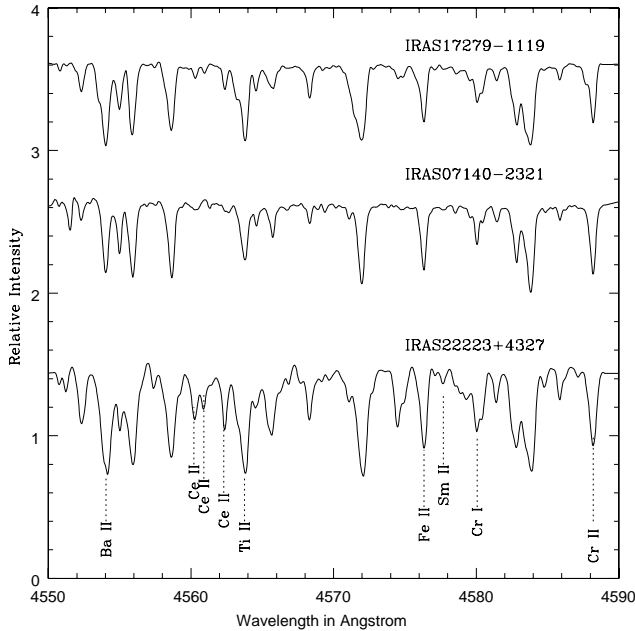


Figure 3. Comparison of spectra of stars IRAS 22223+4327 and IRAS 17279-1119 showing s-process enrichment with IRAS 07140-2321, a normal star of similar temperature in the 4550-4590 Å region. The lines of s-process elements like Ba II, Ce II and Sm II are enhanced.

IR excess is HD 105262 (Giridhar et al. 2010) which has the temperature of 8000K and $[\text{Fe}/\text{H}]$ of -1.8 dex.)

5.12 $[\text{Na}/\text{Fe}]$ in sample stars

The relative enrichment of Na has been observed in most of our program stars. The Na abundance has been measured using weak subordinate lines for which the estimated Non-LTE correction does not exceed -0.1 dex. The Na enrichment is believed to be caused by products of Ne-Na cycle involving proton capture on ^{22}Ne in H burning region which are mixed to the surface following FDU. The verification of expected dependence of $[\text{Na}/\text{Fe}]$ on stellar mass remains illusive. All our program stars give $[\text{Na}/\text{Fe}]$ in excess of FDU predictions (e.g. El Eid and Champagne 1995 predict $[\text{Na}/\text{Fe}]$ of $+0.18$ dex for $5 M_{\odot}$ model). A further increase in surface abundance of Na during AGB evolution is predicted by Mowlavi (1999) but the lack of correlation between the observed $[\text{Na}/\text{Fe}]$ with s-process enhancement cautions against a simplistic interpretation of observed $[\text{Na}/\text{Fe}]$.

5.13 α elements

Our analysis covers whole range of elements including α elements which are important diagnostics of stellar population. Although abundances are estimated for all α elements Mg, Si, S, Ca and Ti, we chose to use only Mg, Si and S to compute $[\alpha/\text{Fe}]$. The Ca and Ti abundances derived from Ca I and Ti I lines could be affected by Non-LTE corrections. For dwarfs and subgiants the corrections are estimated to be about $+0.1$ dex as described in section 4.1, but can become

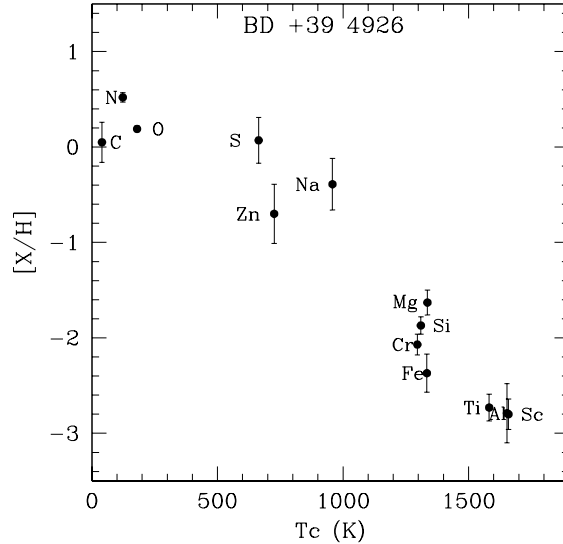


Figure 4. Plot of $[\text{X}/\text{H}]$ vs $[\text{T}_c]$ for the star BD+39°4926.

larger for supergiants. More importantly they are prone to depletion via grain condensation due to their large condensation temperatures (T_c for Ca and Ti are 1517 and 1582K respectively.) As explained in section 4.1, the Non-LTE correction for Mg I lines used by us is about $+0.05$ dex and for S I and Si I lines it is negligible.

The mean $[\alpha/\text{Fe}]$ values of $+0.15$ for IRAS 01259+6823 is indicative of thin disc population, a similar value $+0.18$ for $[\alpha/\text{Fe}]$ is exhibited by IRAS 04535+3747 and $+0.13$ for IRAS 05208-2035 and $+0.21$ is seen for IRAS 17279-1119. The $[\alpha/\text{Fe}]$ of $+0.45$ for IRAS 07140-2321 is indicative of thick disc population; it also shows $[\text{Fe}/\text{H}]$ of -0.9 , IRAS 07331+0021 does not have good representation of α elements. The $[\alpha/\text{Fe}]$ of $+0.36$ for IRAS 08187-1905 and its $[\text{Fe}/\text{H}]$ of -0.6 supports its thick disc candidature. HD 107369 also exhibits $[\alpha/\text{Fe}]$ of $+0.41$ while it is $+0.37$ for IRAS 12538-2611 with $[\text{Fe}/\text{H}]$ of -1.2 . Like other s-process enhanced PAGBs IRAS 22223+4327 exhibits $[\alpha/\text{Fe}]$ value of $+0.46$ not withstanding its $[\text{Fe}/\text{H}]$ of -0.3 . Hence our sample stars are a mixed lot.

5.14 $[\text{Ca}/\text{Fe}]$

For most of our sample stars as well as for a large fraction of RV Tau stars and PAGB stars we find $[\text{Ca}/\text{Fe}]$ and $[\text{Ti}/\text{Fe}]$ much lower than those expected even for thin disc stars. Although Fe abundance can be estimated with better precision using Fe II lines, for Ca, the abundance is estimated using Ca I lines hence Non-LTE corrections for supergiants need to be investigated. (for dwarfs and subgiants $+0.1$ dex is estimated but could be larger for lower gravity PAGB stars). Although this Non-LTE correction for supergiant gravities are not available, it is comforting to note that there is no perceptible difference between $[\text{Ca}/\text{Fe}]$ for a sample of giants

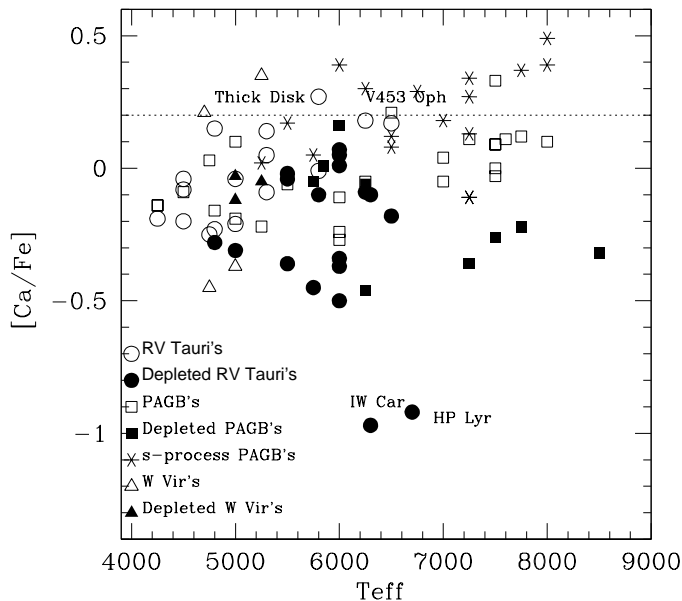


Figure 5. Plot of $[Ca/Fe]$ versus the effective temperature for all groups of PAGB's including our Program Stars.

used by Takeda, Sato and Murata (2008) and those of dwarfs and subgiants (Bensby 2005, Reddy et al. 2006). Hence we do not expect very large reduction in $[Ca/Fe]$ caused by Non-LTE effect (a likely Non-LTE correction would be in +0.1 to 0.2 dex range).

Mild to severe reduction in $[Ca/Fe]$ can be caused by the fact that the T_C for Ca and Fe are 1517K and 1334 respectively, hence Ca is relatively more susceptible to depletion via condensation onto the grains.

To understand $[Ca/Fe]$ variations seen in PAGBs and RV Tau stars a plot of $[Ca/Fe]$ as function of temperature could be instructive notwithstanding the fact that some of the heavily depleted objects do not have Ca measurements and Non-LTE correction could result in at least +0.1dex vertical shift to all data points. The Figure 5 shows thick disc $[Ca/Fe]$ value of +0.21 by dotted horizontal line. The post-AGB stars with s-process enhancement generally have $[Ca/Fe] > 0$. For these objects, α elements including $[Ca/Fe]$ are consistently positive. A few PAGB stars with very mild or no s-process enrichment also show $[Ca/Fe]$ of +0.1 to 0.0. RV Tauris such as V453 Oph showing mild s-process enhancement also show similar $[Ca/Fe]$ values. Depleted PAGBs and RV Tauris understandably show negative $[Ca/Fe]$. IW Car and HP Lyr are well known depleted objects with very small scatter in their T_C vs $[X/H]$ plots. But even those objects with no established indication of dust-gas separation have small negative $[Ca/Fe]$ in excess of what can be ascribed to Non-LTE effects. A large fraction of them have temperatures lower than 5000K, hence the signature of depletion may be muffled for them.

6 DISCUSSION

From the study of extended samples of PAGB stars it has become obvious that they exhibit an enormous chemical variety. However, hardcore PAGB stars showing the predicted outcome of the third dredge-up (increased C/O ratio and s-process enhancements) make a much smaller fraction of known PAGB stars. We have compiled the abundance data for PAGB stars and present them in three tables. We have tabulated separately the PAGB stars showing very distinct s-process enhancement ($[s/Fe] > 0.5$ dex), those showing very distinct depletion of condensable elements (Depletion Index (DI) > 1.0) and those exhibiting neither distinct s-process enhancement nor depletion in an attempt to statistically infer the influence of factors such as binarity, IR fluxes.

6.1 PAGB stars with s-process enhancements

Our compilation of data for PAGB stars with significant s-process enhancements is presented in Table 9. A few stars have more than one analysis. Most analyses employ resolution around 40,000. More recent analyses employ more accurate oscillator strengths. It should be noted that a majority of them belong to thick disc population with $[Fe/H]$ in range -0.3 to -0.8 dex. Early discoveries of this class with large $[s/Fe]$ led to phrase "have" meaning members with $[s/Fe]$ in range $+1.5$ to $+2.3$ and "have not" with $[s/Fe] \sim 0$.

However, recent studies (including the present work) have found the objects with moderate s-process enhancements and C/O not exceeding one. Heavily enriched objects seem to favour a temperature range of 6000K to 7500K. They all have $[\alpha/Fe]$ in similar to those of thick disc stars. A large fraction of them show 21μ feature. The SED generally contains well resolved IR component of strength comparable to photospheric component. Three objects from Table 9 IRAS 08143-4406, IRAS 22223+4327 and IRAS 23104+6147 have nebulae of SOLE class (generally of 2 arcsec size) detected by Siódmiak et al. (2008). Another interesting feature of this class of s-process enhanced PAGB stars is that very few of them are known binaries. They appear to represent single star evolution of moderately metal-poor thick disc stars.

6.2 PAGB stars with depletion of refractory elements

Although a working hypothesis of dust-gas separation in circumbinary disc causing selective depletion of refractory elements has been proposed, the actual mechanism of disc formation and its evolution is far from understood.

We have compiled the existing data for all known PAGB stars and RV Tau stars and chosen very stringent selection criteria to define the group of PAGB stars showing depletion due to selective removal of condensable elements. The guideline being $[S/Fe]$ and $[Zn/Fe] > 0$ and $[Ca/Fe]$, $[Sc/Fe]$, $[Ti/Fe] < 0.0$. We present our compilation in Table 10. It is possible that adherence to this criteria would result in non-inclusion of some PAGB stars considered mildly depleted in other studies.

Quantifying the depletion process is a very difficult task. S and Zn are good representatives of non-depleted elements

Table 9. A list of post-AGB stars with enhancement of s-process elements

IRAS	Other names	T _{eff}	[Fe/H]	[α /Fe]	[s/Fe]	[ls/Fe]	[hs/Fe]	[hs/ls]	Ref	Binarity
08281-4850	...	7750	-0.33	+0.25	+1.24	+1.23	+1.25	+0.02	8	No
22223+4327	BD+42°4388, V448 Lac	6500	-0.33	+0.25	+0.92	+1.31	+1.18	-0.13	1	No
...	...	6750	-0.30	+0.24	+1.08	+1.36	+0.94	-0.42	9	No
08143-4406	...	7250	-0.39	+0.24	+1.51	+1.53	+1.50	-0.02	2	No
06530-0213	...	7250	-0.46	+0.20	+2.06	+1.83	+2.18	+0.35	2	No
17279-1119	HD 158616, V340 Ser	7250	-0.43	+0.25	+0.64	+0.70	+0.62	-0.08	1	No
...	...	7300	-0.60	+0.44	+0.69	+0.95	+0.60	-0.35	5	No
...	...	7400	-0.68	+0.78	+0.50	+0.50	..	-0.50	6	No
Z02229+6208	...	5500	-0.50	+0.17	+1.37	+2.08	+1.13	-0.95	4	No
07430+1115	...	6000	-0.50	+0.09	+1.60	+2.09	+1.44	-0.65	4	No
14325-6428	...	8000	-0.55	+0.30	+1.25	+1.23	+1.29	+0.06	8	No
18384-2800	HD 172481, V4728 Sgr	7250	-0.62	+0.46	+0.48	+0.58	+0.44	-0.14	5	Yes
...	...	7250	-0.55	+0.37	+0.48	+0.49	+0.47	-0.02	9	Yes
04296+3429	...	7000	-0.65	+0.38	+1.55	+1.66	+1.49	-0.17	9	No
19500-1709	HD 187885, V5112 Sgr	8000	-0.66	+0.30	+1.15	+1.40	+1.03	-0.37	9	No
...	...	8000	-0.44	+0.54	+1.31	+1.29	+1.35	+0.06	7	No
05341+0852	...	6500	-0.72	+0.29	+2.22	+2.01	+2.32	+0.32	9	No
05113+1347	...	5250	-0.75	+0.18	+2.00	+1.61	+2.16	+0.55	3	No
23304+6147	...	6750	-0.81	+0.32	+1.60	+1.55	+1.63	+0.09	9	No
22272+5435	HD 235858, V354 Lac	5750	-0.82	+0.17	+1.99	+1.56	+2.17	+0.61	3	No
07134+1005	HD 56126, CY CMi	7250	-1.03	+0.08	+1.51	+1.56	+1.49	-0.06	9	No

¹Present work., ²Reyniers et al. 2004, ³Reddy et al. 2002, ⁴Reddy et al. 1999

⁵Arellano Ferro et al. 2001, ⁶Van Winckel et al. 1997, ⁷Van Winckel et al. 1996

⁸Reyniers et al. 2007, ⁹Reyniers (2002)

due to their low condensation temperatures 704 and 726K respectively. CNO inspite their lower T_C are not useful since they are affected by nuclear processing and dredge-ups. However Zn I lines are strongest at around 4700K and remain strong at even lower temperatures but the spectrum gets too crowded to measure them. At higher temperatures like 7000K and above they become weak and are weaker than 10 mÅ at 8000K. The lines of S I are at the strongest near 6700K but weaken drastically at cooler as well as hotter temperatures. Hence the abundance errors are highly temperature dependent. We have taken mean of heavily depleted elements Ca, Sc and Ti (with similar condensation temperatures 1517, 1582 and 1659K respectively) and subtracted it from [S/H] to define depletion index given in Table 10. Ideally [Al/H] should have been included in the calculations, but Al abundances were not available for many stars. For a few stars only two of these three elements are measured; then the mean is taken of the elements for which data is available. For heavily depleted stars [Zn/H] is a better metallicity indicator; hence the objects with [Zn/H] < -0.5 dex could belong to thick disc and halo population.

We have studied T_C vs [X/H] curves for all stars of Table 10 and have indicated by * those that exhibit very smooth curves like HP Lyr in the column for DI (Depletion Index).

The compilation brings about intriguing statistics; out of 36 depleted PAGB stars 25 are known binaries, 28 have IRAS detections seven are without (which is about 19%).

Hence it is obvious that binarity plays very important role. Non detection of IRAS fluxes could be caused by weakening and cooling of the disc hence surveys at longer wave-

lengths and with increased sensitivities are required to resolve this issue.

However there are objects like IRAS 07140-2321 which has dusty CS, known to be a binary with period of 116 days and yet does not show the depletion! The boundary conditions suggested in scenarios proposed to explain these phenomenon deserve a close scrutiny.

In our study of extended sample for RV Tau stars (Giridhar et al. 2005) we had proposed two scenarios (based upon the single star and binary configuration) and also discussed the parameters strongly affecting the depletion caused by dust-gas separation.

- **The surface temperature:** The first important requirement was that the star must be hotter than ~ 5000K. The cooler RV Tau stars (RVA) did not show the abundance anomalies, possibly their massive convective envelopes diluted the effect of accreted gas which was cleaned of refractory elements. The masses of convective envelopes for PAGB stars increases with decreased temperature (see Frankowski 2003 for more details) varies from 0.016 M_⊙ at 4000K to 0.0001 M_⊙ at 6000K. At 6000K the mass of convective envelope is about 1000 times that of observable photosphere. At hot temperature the abundance deficiency of readily condensable elements (those with high T_c) may approach a thousandfold and in such cases the surface and convective envelope would be composed of almost undiluted accreted gas. At lower temperatures, in addition to larger convective mass the stronger stellar wind may oppose the accretion of the clean gas.

- **The metallicity:** The dust-gas separation process has not been seen in stars with intrinsic metallicity lower than ~ -1.0 irrespective of their temperatures. It is likely conse-

Table 10. A list of post-AGB stars showing depletion

IRAS	Other ^a	T _{eff}	[12]-[25]	[25]-[60]	[S/H]	[Zn/H]	[Ca/H]	[Sc/H]	[Ti/H]	[Fe/H]	DI ^b	Ref	Bin ^c
...	TT Oph	4800	+0.01	-0.71	-1.13	-1.09	-0.82	-0.85	1.02	2	N
...	UZ Oph	5000	-0.38	-0.74	-1.10	-1.26	-1.00	-0.79	1.50	4	N
...	W Vir	5000	-0.26	-0.84	-1.03	-2.03	-1.08	-1.00	1.12	12	N
...	V1711 Sgr	5000	-0.07	-0.98	-1.32	-2.46	-2.05	-1.20	1.87	12	N
...	RX Lib	5250	-0.58	-0.80	-1.05	-2.22	-1.14	-1.00	0.89	12	N
17250-5951	UY Ara	5500	+0.27	-0.95	+0.01	-0.29	-1.06	-1.74	..	-1.02	1.41*	2	N
06054+2237	SS Gem	5500	-0.28	+0.08	-0.42	+0.02	-1.05	-1.92	-2.00	-0.87	1.24	3	N
06072+0953	CT Ori	5500	-0.11	-1.63	-0.53	-0.58	-1.80	-2.58	-2.51	-1.87	1.65*	3	Y
06160-1701	UY CMa	5500	-0.38	-1.59	-0.32	-0.59	-1.65	-2.22	-2.38	-1.29	1.65*	4	Y
20117+1634	R Sge	5750	-0.37	-1.38	+0.37	-0.19	-0.95	-1.48	-1.34	-0.50	1.63	5	Y
19163+2745	EP Lyr	5750	+0.52	-0.24	-0.61	-0.70	-1.82	-2.11	-2.01	-1.80	1.26*	5	Y
09144-4933	..	5750	-0.25	-1.57	-0.01	..	-0.37	-1.65	-1.28	-0.31	1.09	14	N
20056+1834	QY Sge	5850	+0.03	-1.31	+0.14	-0.14	-0.28	-0.70	-1.15	-0.29	0.85	13	Y
07008+1050	HD 52961	6000	-0.77	-0.92	-1.00	-1.40	-4.80	3.80†	8	Y
06338+5333	HD 46703	6000	-0.21	+0.05	-0.40	-1.40	-1.60	..	-1.79	-1.60	1.00*	11	Y
18281+2149	AC Her	6000	+0.50	-1.21	-0.37	-0.93	-1.50	-1.70	-1.64	-1.40	1.13*	6	Y
08011-3627	AR Pup	6000	-0.36	-1.39	+0.44	..	-1.37	-2.16	..	-0.87	2.20	5	Y
06034+1354	DY Ori	6000	+0.19	-1.38	+0.16	+0.21	-1.70	..	-2.33	-2.30	2.65*	4	Y
12067-4508	RU Cen,	6000	+0.78	-0.72	-0.68	-1.00	-1.89	-1.88	-1.96	-1.90	1.11	7	Y
18548-0552	BZ Sct	6250	+0.05	+0.49	+0.18	+0.04	-0.91	-1.13	-1.22	-0.82	1.27	4	N
...	CC Lyr	6250	-0.50	-1.20	-3.40	2.90†	12	N
16230-3410	...	6250	-0.27	-1.52	-0.36	-0.42	-0.74	-2.28	-1.45	-0.68	1.13	14	Y
17233-4330	...	6250	-0.26	-1.40	+0.14	-0.21	-1.39	-1.60	-1.62	-0.98	1.68	14	Y
17243-4348	LR Sco	6250	-0.22	-0.94	+0.04	+0.22	-0.17	-1.11	-0.61	-0.05	1.07	4	Y
18564-0814	AD Aql	6300	+0.09	-1.55	-0.03	-0.12	-2.22	-1.79	-2.57	-2.12	2.16*	6	Y
19199+3950	HP Lyr	6300	-0.02	-1.56	+0.05	-0.35	-1.95	-2.87	-2.97	-0.98	2.83*	4	N
12185-4856	SX Cen	6500	-0.54	-1.28	-0.08	-0.54	-1.52	-1.96	-1.97	-1.15	1.62	7	Y
09256-6324	IW Car,	6700	-0.05	-1.11	+0.36	-0.04	-1.97	-2.13	..	-1.0	2.41*	10	Y
08544-4431	V390 Vel	7250	-0.14	-1.13	+0.12	+0.09	-0.36	-0.87	-0.85	-0.50	0.81*	15	Y
15469-5311	..	7500	-0.16	-1.08	+0.51	+0.25	-0.46	-1.56	-1.57	+0.04	1.70	14	Y
10158-2844	HR 4049	7500	-1.76	-1.83	-0.40	-1.30	-5.30	-4.80	4.90*	8	Y
06176-1036	HD 44179	7500	+0.09	-1.05	-0.30	-0.60	-3.11	-3.30	2.69*	8	Y
19125+0343	BD+03°3950	7750	-0.09	-1.32	+0.48	+0.13	-0.51	..	-2.15	-0.35	1.75*	14	Y
...	BD+39°4926	7750	+0.07	-0.70	..	-2.80	-2.73	-2.37	2.72*	1	Y
22327-1731	HM Aqr	8200	-0.19	-0.86	+0.36	-1.31	-1.49	-0.90	1.76	8	Y
...	HD 105262	8500	-0.50	..	-2.10	-2.07	-1.58	-1.90	1.42*	9	Y

^aOther refers to other names.

^bDI refers to Depletion Index. † refers to D.I measured from S and Fe in absence of other elements. * indicate that the depletion plots of these stars had less scatter.

^cBin refers to Binarity.

¹Present work., ²Giridhar et al. 2000, ³Guillermo Gonzalez et al. 1997a, ⁴Giridhar et al. 2005

⁵Guillermo Gonzalez et al. 1997b, ⁶Giridhar et al. 1998, ⁷Maas et al. 2002, ⁸Van Winckel (1995)

⁹Giridhar et al. 2010, ¹⁰Giridhar et al. 1994, ¹¹Hrivnak et al. 2008,

¹⁰Giridhar et al. 1994, ¹¹Hrivnak et al. 2008, ¹²Maas et al. 2007

¹³Rao et al. 2002, ¹⁴Maas et al. 2005, ¹⁵Maas et al. 2003

quence of the inability of radiation pressure on dust grains to force a separation of dust from gas when the mass fraction of the dust is very low as seen in metal-poor environments. A dust-gas reservoir with metallicity in excess of -1.0 is mandatory for efficient separation of dust from the gas. These conditions can be easily realized in binary scenario with circumbinary disc since it may contain gas from either binary companion or the main star before the onset of accretion.

Although a revised minimum temperature 4800K for

discernible depletion has been identified, but stars in temperature range 6000K to 7500K tend to show large depletions. At hotter side $T_{eff} > 8500$ K DI is smaller; a shift in ionization structure causing the observable features to become too scarce for S and Zn may be responsible.

Many stars such as CC Lyr, HR 4049, BD+39°4926 show large differences between S and Zn despite these elements having nearly the same T_C . For thick disc and halo stars relative enrichment of S by +0.3 dex can be anticipated since the S is an α element but for larger differences found in the above mentioned objects there is no ready explanation.

Table 11. A list of post-AGB stars showing neither significant s-process enrichment nor depletion

IRAS	Other ^a	T _{eff}	[12]-[25]	[25]-[60]	[S/H]	[Zn/H]	[Ca/H]	[Sc/H]	[Ti/H]	[Fe/H]	Ref	Bin ^b	
02008+4205	HD 12533	4250	-1.55	-2.05	..	-0.05	-0.20	-0.08	-0.21	-0.06	8	N	
19437-1104	DY Aql	4250	+0.17	-0.37	-1.22	-2.13	..	-1.03	3	N	
20343+2625	V Vul	4500	-0.84	-1.60	+0.57	-0.27	-0.47	-0.69	-0.18	-0.39	1	Y	
18448-0545	R Sct	4500	-0.89	-0.14	..	-0.19	..	-1.43	-0.38	-0.35	2	N	
04440+2605	RV Tau	4500	-0.24	-1.11	..	+0.02	-0.48	-0.35	-0.53	-0.40	2	Y	
07331+0021	AI CMi	4500	+1.62	-1.42	-1.25	-1.35	-0.89	-1.16	11	N	
06489-0118	SZ Mon	4700	-0.54	-1.38	+0.24	-0.43	-0.19	-1.46	-1.25	-0.40	10	N	
...	MZ Cyg	4750	+0.53	-0.23	-0.65	-1.07	-0.63	-0.20	10	N	
...	AZ Sgr	4750	-0.34	..	-1.80	-1.78	-1.57	-1.55	1	N	
17038-4815	..	4750	+0.19	-0.84	-1.20	-1.47	-2.00	-1.40	-1.50	6	Y
17193+8439	HD 159251	4800	-1.27	+0.99	..	-0.14	-0.21	-0.03	-0.10	-0.05	8	N	
19472+4254	DF Cyg	4800	-0.65	-0.82	..	-0.62	-0.23	-0.96	-0.04	+0.00	1	N	
04166+5719	TW Cam	4800	-0.42	-1.20	-0.05	-0.34	-0.65	-0.43	-0.64	-0.50	2	Y	
07284-0940	U Mon	5000	-0.37	-1.31	-0.15	-0.71	-0.96	-0.97	-0.70	-0.79	2	Y	
F17015+0503	TX Oph	5000	-0.63	-1.23	-1.43	-1.79	-1.18	-1.22	1	N	
01369+4124	HD 10132	5000	-0.62	+0.02	+0.15	-0.14	+0.05	+0.36	-0.02	-0.05	8	N	
...	CO Pup	5000	-0.05	-0.73	-0.97	-1.56	-0.94	-0.60	10	N	
...	TW Cap	5250	-1.40	-1.52	-1.45	-1.61	-1.42	-1.80	10	N	
...	V360 Cyg	5250	-0.88	-1.36	-1.26	..	-1.28	-1.40	4	N	
17530-3348	AI Sco	5300	-0.47	-1.46	-0.08	-0.61	-0.64	-0.96	-0.89	-0.69	1	Y	
...	AR Sgr	5300	-0.82	-1.20	-1.44	-1.41	-1.21	-1.33	1	N	
09538-7622	...	5500	-0.40	-1.20	-0.30	-0.60	-0.66	-0.90	-0.70	-0.60	6	Y	
...	RX Cap	5800	-0.57	-0.63	-0.79	-1.20	-0.62	-0.78	1	N	
...	BT Lib	5800	-0.76	-1.06	-0.91	-0.71	-0.96	-1.18	2	N	
04535+3747	V409 Aur	6000	-0.73	-0.03	-0.16	-0.53	-0.59	-0.75	-0.63	-0.48	11	N	
13110-5425	HD 114855	6000	+2.08	+1.39	+0.34	-0.26	-0.35	-0.34	-0.41	-0.11	5	N	
14524-6838	EN TrA	6000	-0.28	-0.99	-0.61	-0.56	-1.03	..	-1.11	-0.76	7	Y	
08187-1905	V552 Pup	6250	+ 3.49	-0.39	+0.05	-0.58	-0.63	-0.75	-0.99	-0.59	11	N	
09060-2807	BZ Pyx	6500	-0.43	-1.46	-0.70	-0.50	-0.49	-0.80	-0.70	-0.70	6	Y	
...	DS Aqr	6500	-0.82	-1.07	-0.97	-1.17	..	-1.14	2	N	
12222-4652	HD 108015	7000	+0.03	-1.55	-0.15	-0.16	-0.05	-0.80	-0.26	-0.09	7	Y	
IRAS 07140-2321	SAO 173329	7000	-0.24	-1.14	-0.32	-0.87	-0.97	-0.92	-0.73	-0.92	11	Y	
04002+5901	HD 25291	7250	-1.46	-0.02	+0.08	..	-0.22	+0.01	-0.30	-0.33	8	N	
07018-0513	HD 53300	7500	-0.97	+0.30	-0.04	-0.71	-0.62	-0.96	-0.83	-0.62	5	N	
18439-1010	HD 173638	7500	-1.38	+0.59	..	-0.06	+0.01	+0.16	-0.05	-0.08	9	N	
12175-5338	SAO 239853	7500	+3.25	-1.08	-0.40	-0.73	-0.48	-1.11	-0.54	-0.81	7	N	
04175+3827	HD 27381	7500	-0.99	+0.24	-0.30	..	-0.59	-0.39	-0.57	-0.67	8	N	
...	HD 107369	7500	-0.84	..	-1.36	-1.45	-1.09	-1.33	11	N	
11000-6153	HD 95767	7600	-0.37	-0.39	+0.01	-0.12	+0.24	..	-0.11	+0.13	7	Y	
19157-0247	...	7750	-0.23	-1.17	+0.20	-0.40	-0.20	+0.10	6	Y	
...	HD 10285	7750	+0.04	-0.36	-0.19	-0.07	-0.30	-0.31	8	N	
...	HD 218753	8000	+0.17	+0.18	-0.09	+0.00	-0.26	-0.19	9	N	

^aOther refers to other names, ^bBin refers to Binarity.

¹Giridhar et al. 2005, ²Giridhar et al. 2000, ³Guillermo Gonzalez et al. 1997a, ⁴Giridhar et al. 1998

⁵Giridhar et al. 2010, ⁶Maas et al. 2005, ⁷Van Winckel (1996), ⁸Giridhar & Arellano Ferro (2005)

⁹Arellano Ferro et al. 2001, ¹⁰Maas et al. 2007, ¹¹Present Work

Another intriguing observation is that DI are not correlated with IRAS colours nor do they show any correlation with IR flux at a given wavelength.

Since the SED characteristics can be used to develop a model for circumstellar material, De Ruyter et al. (2006) have done optical photometry and have also used the IR and sub-millimeter data for a large sample of known binary PAGB stars and other objects (like RV Tau stars) of similar IR characteristics. Using the optically thin dust model they found the dust at or near sublimation temperature (1200K) and also very close to the star (~ 10 AU from the central source) irrespective of the effective temperature of the star.

These authors argued that at least a part of the dust must be gravitationally bound since any typical AGB outflow velocity would bring the dust to cooler region within years. Although their sample of known PAGB binary and RV Tau stars of similar characteristics had a large range in the size of IR excess, but the shape of IR excess indicated that CS was not freely expanding but was stored in the system. A study of orbital parameters for the well-studied objects point to orbits which are too compact for sizes of PAGB stars. These authors further suggest that it is highly improbable that these stars have evolved as single stars; a strong interaction

phase while the star was in giant stage is required to explain the present configuration.

The high spatial resolution interferometry in mid IR has been used to resolve compact dusty discs around the depleted binary post-AGB stars. For Red Rectangle, HR 4049 and recently for HD 52961 the dusty discs have been resolved (Deroo et al. 2007). It is comforting to see the additional information provided by high spatial resolution interferometry towards better understanding of these systems but the accuracies of disc dimensions are constrained by the radiative transfer models.

6.3 PAGB stars without significant s-process enhancement nor showing depletions

A good number of PAGB candidates displaying basic PAGB characteristics like IRAS colours, high luminosity, small amplitude light and radial velocity variations do not belong to the above mentioned classes. Regarding s-process enhancements, the earlier samples of PAGB belonged to only two classes "have" and "have not"; the "have" showing strong s-process enhancements ($[s/Fe] > 1$) while many of the "have nots" had subsolar $[s/Fe]$ ratios. With increased sample the moderately enhanced members are making an appearance. IRAS 17279-1119 has been known for some time but IRAS 01259+6823, IRAS 05208-2035 and IRAS 08187-1905 are new additions.

Then there are other PAGB stars including RV Tauris without significant s-process enhancement nor showing depletions. We have tabulated 42 such objects (more than half are RV Tauris and Semi-regular variable of type D SRDs) in Table 11. A large fraction of them (30) are IRAS sources, One fourth (13) are binaries all showing IRAS fluxes. In terms of temperature range and IRAS colours they are indistinguishable from those in Table 10. PAGB with s-process enhancements (Table 9) appear to be systematically warmer. It should be noted that larger DI PAGB also seem to favour the same temperature range. Then it would appear that condition of low surface temperature are not conducive for the survival of abundance peculiarities although unglamorous objects are found even in among objects in temperatures range of 6000K to 7500K.

7 SUMMARY

In our exploration of post-AGB candidates we find mild enhancements of s-process elements in IRAS 01259+6823, IRAS 05208-2035 and IRAS 08187-1905, while significant enhancement is found for IRAS 17279-1119 and IRAS 22223+4327. Mild s-process enhancement and low temperatures of IRAS 05208-2035 and IRAS 01259+6823 are not of common occurrence in post-AGB stars although the theory does not prohibit such objects since the degree of s-process enhancement gradually builds with number of thermal pulses. However further evidence like intrinsic luminosity estimates are awaited.

A survey of well established s-process enhanced post-AGB stars shows majority of this group to be most likely thick disc objects of intermediate temperatures. It does not appear that their evolution is strongly affected by the presence of binary companion. Most of these heavily s-processed

objects have temperatures between 6000K to 7500K, although a spread in $[s/Fe]$ for similar atmospheric parameters is seen indicating the influence of additional processes on third dredge-up efficiency.

A contemporary analysis of BD+39° 4926 has been conducted and initial metallicity of -0.7 dex has been estimated. HD 107369 appear to be a metal-poor, high galactic latitude supergiant with strong influence of CN processing. The observed N enhancement is in excess of that predicted by the FDU but cannot be ascribed to large rotation at main sequence as the stellar lines are very sharp and narrow – not much broader than the instrumental profile.

Our compilation of the PAGB stars showing the abundance peculiarities caused by selective depletion of refractory elements reiterates the temperature and metallicity limits observed earlier for their detection. The observed spectral energy distribution with dust excess of these objects have been interpreted by De Ruyter et al. 2006 via a circumstellar dust shell contained in Keplerian rotating discs. But the actual resolution of dusty discs and measurement of their sizes has been possible only for heavily depleted objects like HR 4049, Red Rectangle and more recently HD 52961 although HD 52961 does not exhibit large IR excess. Search of such depleted objects and their follow-up using high spatial resolution mid IR interferometry and IR spectroscopy can provide valuable insight into the circumstellar geometries of these objects.

Our compilation of PAGB stars showing neither of these two peculiarities is indistinguishable from these two samples in terms of basic stellar parameters. Hence the cause separating these subgroups among PAGB stars is not understood.

The extension of abundance analysis to PAGB candidates located in uniform stellar system such as globular clusters, or in neighbouring galaxies would help since each system would have small range in mass and metallicity.

ACKNOWLEDGMENTS

DLL thanks the Robert A. Welch Foundation of Houston, Texas for support through grant F-634.

REFERENCES

- Aldenius, M., Lundberg, H., Blackwell-Whitehead, R., 2009, *A&A*, 502, 989
- Allen, D. M., Porto de Mello, G. F., 2011, *A&A*, 525, 63
- Arellano Ferro, A., Giridhar, S., Mathias, P., 2001, *A&A*, 368, 250
- Arkhipova, V. P., Noskova, R. I., Ikonnikova, N. P., Komissarova, G. V., 2003, *Astronomy Letters*, 29, 480
- Asplund, M., Grevesse, N., Sauval, A. J., 2005, *ASP Conf.Ser.*336, 25
- Bensby, T., Feltzing, S., Lundström, I., Ilyin, I., 2005, *A&A*, 433, 185
- Bergemann, M., Cescutti, G., 2010, *A&A*, 522, A9
- Bergemann, M., 2011, *MNRAS*, 413, 2184
- Biémont, E., Grevesse, N., Hannaford, P., Lowe, R. M., 1981, *ApJ*, 248, 867
- Bogaert, E., Ph.D. Thesis, K.U. Leuven, 1994
- Boyarchuk, A. A., Lyubimkov, L. S., Sakhbullin, N. A., 1985, *Astrophysics*, 22, 203
- Böcker, T., Schönberner, D., 1991, *A&A*, 244, L43

- Curry, J. J., 2004, *J. Phys. Chem. Ref. Data*, 33, 725
- Den Hartog, E. A., Lawler, J. E., Sneden, C., Cowan, J. J., 2003, *ApJS*, 148, 543
- Deroo, P., Ache, B., Verhoelst, T., Dominik, C., Tatulli, E., Van Winckel, H., 2007, *A&A*, 474, 45
- De Ruyter, S., Van Winckel, H., Maas, T., Llyod Evans, T., Waters, L. B. F. M., Dejonghe, H., 2006, *A&A*, 448, 641
- El Eid, M. F., Champagne, A. E., 1995, *ApJ*, 451, 298
- Frankowski, A., 2003, *A&A*, 406, 265
- Fuhr, J. R., Martin, G. A., Wiese, W. L., 1988, *J. Phys. Chem. Ref. Data*, 4, 493
- Fuhr, J. R., Wiese, W. L., 2005, *CRC Handbook of Chemistry and Physics*, 86th Edition
- Fuhr, J. R., Wiese, W. L., 2006, *J. Phys. Chem. Ref. data*, 35, 1669
- Gehren, T., Liang, Y. C., Shi, J. R., Zhang, H. W., Zhao, G., 2004, *A&A*, 413, 1045
- Gielen, C., Van Winckel, H., Min, M., Waters, L. B. F. M., Lloyd Evans, T., 2008, *A&A*, 490, 725
- Giridhar, S., Rao, N. K., Lambert, D. L., 1994, *ApJ*, 437, 476
- Giridhar, S., Arellano Ferro, A., Parrao, L., 1997, *PASP*, 109, 1077
- Giridhar, S., Lambert, D. L., Guillermo Gonzalez, 1998, 509, 366
- Giridhar, S., Lambert, D. L., Guillermo Gonzalez, 2000, *ApJ*, 531, 521
- Giridhar, S., Arellano Ferro, A., 2005, *A&A*, 443, 297
- Giridhar, S., Lambert, D. L., Reddy, B. E., Guillermo Gonzalez., David Yong., 2005, *ApJ*, 627, 432
- Giridhar, S., Molina, R., Arellano Ferro, A., Selvakumar, G., 2010, *MNRAS*, 406, 290
- Guillermo Gonzalez, Lambert, D. L., Giridhar, S., 1997a, *ApJ*, 481, 452
- Guillermo Gonzalez, Lambert, D. L., Giridhar, S., 1997b, *ApJ*, 479, 427
- Hannaford, P., Lowe, R. M., Grevesse, N., Biéumont, E., Whaling, W., 1982, *ApJ*, 261, 736
- Herwig, F., 2005, *ARA&A*, 43, 435
- Hrivnak, J., 1995, *ApJ*, 438, 341
- Hrivnak, B. J., Van Winckel, H., Reyniers, M., Bohlender, D., Waelkens, C., Wenxian Lu., 2008, *AJ*, 136, 1557
- Kelleher, D. E., Podobedova, L. I., 2008a, *J. Phys. Chem. Ref. Data*, 37, 267
- Kelleher, D. E., Podobedova, L. I., 2008b, *J. Phys. Chem. Ref. Data*, 37, 709
- Kelleher, D. E., Podobedova, L. I., 2008c, *J. Phys. Chem. Ref. Data*, 37, 1285
- Kiss, L. L., Derekas, A., Szabó, M., Bedding, T. R., Szabados, L., 2007, *MNRAS*, 375, 1338
- Klochkova, V. G., Panchuk, V. E., 1996, *Bull.Spec.Astrophys.Obs*, 41, 5
- Klochkova, V. G., Panchuk, V. E., 1998, *Astronomy Letters*, 24, 650
- Klochkova, V. G., Panchuk, V. E., Tavalzhanskaya, N. S., 2010, *Astronomy Reports*, 54, 234
- Kodaira, K., Greenstein, J. L., Oke, J. B., 1970, *ApJ*, 159, 485.
- Korotin, S. A., 2009, *Astronomy Reports*, 53, 651
- Kwok, S., 1993, *ARA&A*, 31, 63
- Kurucz, R.L., Furenlid, I., Brault, J., Testerman, L., 1984, *National Solar Observatory Atlas, Sunspot, New Mexico: National Solar Observatory*
- Lawler, J. E., Bonvallet, G., Sneden, C., 2001a, *ApJ*, 556, 452
- Lawler, J. E., Wickliffe, M. E., Den Hartog, E. A., Sneden, C., 2001b, *ApJ*, 563, 1075
- Lawler, J. E., Den Hartog, E. A., Sneden, C., Cowan, J. J., 2006, *ApJS*, 162, 227
- Lawler, J. E., Sneden, C., Cowan, J. J., Ivans, I. I., Den Hartog, E. A., 2009, *ApJS*, 182, 51
- Lind, K., Asplund, M., Barklem, P. S., Belyaev, A. K., 2011, *A&A*, 528, 103
- Luck, R. E., Lambert, D. L., Bond, H. E., 1983, *PASP*, 98, 413
- Luck, R.E., Bond, H.E., 1989, *ApJ*, 342, 476
- Lyubimkov, L. S., Lambert, D. L., Korotin, S. A., Poklad, D. B., Rachkovskaya, T. M., Rostopchin, S. I., 2011, *MNRAS*, 410, 1774
- Maas, T., Van Winckel, H., Waelkens, C., 2002, *A&A*, 386, 504
- Maas, T., Van Winckel, H., Llyod Evans, T., Nyman, L. Å., Kilkeny, D., Martinez, P., Marang, F., van Wyk, F., 2003, *A&A*, 405, 271
- Maas, T., Van Winckel, H., Evans, L. T., 2005, *A&A*, 429, 297
- Maas, T., Giridhar, S., Lambert, D. L., 2007, *ApJ*, 666, 378
- Martin, G. A., Fuhr, J. R., Wiese, W. L., 1988, *J. Phys. Chem. Ref. Data*, 3, 512
- Mashonkina, L., Korn, A. J., Przybilla, N., 2007, *A&A*, 461, 261
- Mashonkina, L., 2011, arXiv:1104.4403
- McWilliam, A., 1998, *AJ*, 115, 1640
- Meléndez, J., Barbuy, B., 2009, *A&A*, 497, 611
- Mowlavi, N., 1999, *A&A*, 350, 73
- Mucciarelli, A., Caffau, E., Freytag, B., Hans-Günter Ludwig, Bonifacio, P., 2008, *A&A*, 484, 841
- Podobedova, L. I., Kelleher, D. E., Wiese, W. L., 2009, *J. Phys. Chem. Ref. Data*, 38, 171
- Prochaska, J. X., McWilliam, A., 2000, *ApJ*, 537, 57
- Rao, N. K., Goswami, A., Lambert, D. L., 2002, *BASI*, 30, 671
- Rao, N. K., Reddy, B. E., 2005, *MNRAS*, 357, 235
- Reddy, B. E., Parthasarathy, M., 1996, *AJ*, 112, 2053
- Reddy, B. E., Bakker, E. J., Hrivnak, B. J., 1999, *ApJ*, 524, 831
- Reddy, B. E., Guillermo Gonzalez., David Yong, 2002, *ApJ*, 564, 482
- Reddy, B. E., Lambert, D. L., Allende Prieto, C., 2006, *MNRAS*, 367, 1329
- Reyniers, M., 2002, Ph.D Thesis, K. U. Leuven
- Reyniers, M., Van Winckel, H., Gallino, R., Straniero, O., 2004, *A&A*, 417, 269
- Reyniers, M., Van de Steene, G. C., Van Hoof, P. A. M., Van Winckel, H., 2007, *A&A*, 471, 247
- Romano, D., Karakas, A. I., Tosi, M., Matteucci, F., 2010, *A&A*, 522, A32
- Sansonetti, J. E., 2008, *J. Phys. Chem. Ref. Data*, 37, 1659
- Schaller, G., Schaerer, D., Mainer, G., Maeder, A., 1992, *A&AS*, 96, 269
- Schiller, F., Przybilla, N., 2008, *A&A*, 479, 849
- Siódmiak, N., Meixner, M., Ueta, T., Sugeran, B. E. K., Van de Steene, G. C., Szczerba, R., 2008, *ApJ*, 677, 382
- Sneden, C., 1973, Ph.D Thesis, Univ. of Texas at Austin, USA
- Sneden, C., Lawler, J. E., Cowan, J. J., Ivans, I. I., Den Hartog, E. A., 2009, *ApJS*, 182, 80
- Sobeck, J. S., Lawler, J.E., Sneden, C., 2007, *ApJ*, 667, 1267
- Suárez, O., García-Lario, P., Manchado, A., Manteiga, M., Ulla, A., Pottasch, S. R., 2006, *A&A*, 458, 173
- Szczerba, R., Siódmiak, N., Stasińska, G., Borkowski, J., 2007, *A&A*, 469, 799
- Takeda, Y., Takada-Hidai, M., 1998, *PASJ*, 50, 629
- Takeda, Y., Sato, B., Murata, D., 2008, *PASJ*, 60, 781
- Thévenin, F., Idiart, T. P., 1999, *ApJ*, 521, 753
- Tull, R. G., MacQueen, P. J., Sneden, C., Lambert, D. L., 1995, *PASP*, 107, 251
- van der Veen, W. E. C. J., Habing, H. J., 1988, *A&A*, 194, 125
- Van Winckel, H., 1995, Ph.D Thesis, K. U. Leuven
- Van Winckel, H., 1996, *A&A*, 319, 561
- Van Winckel, Waelkens, C., Waters, L. B. F. M., 1996, *A&A*, 306, 37
- Van Winckel, H., 1997, *A&A*, 319, 561
- Van Winckel, H., Reyniers, M., 2000, *A&A*, 354, 135
- Van Winckel, H., Waelkens, C., Waters, L. B. F. M., 2000, *IAUS*, 177, 285

- Van Winckel, H., 2003, *ARA&A*, 41, 391
Velichko, A. B., Mashonkina, L. I., Nilsson, H., 2010, *Astronomy Letters*, 36, 664
Venn, K.A., 1995, *ApJ*, 449, 839.
Ventura, P., D'Antona, F., 2009, *A&A*, 499, 835
Wedemeyer, S., 2001, *A&A*, 373, 998
Wiese, W. L., Fuhr, J. R., Deters, T. M., 1996, *J. Phy. Chem. Ref. Data*, Monograph No. 7
Wiese, W. L., Fuhr, J. R., 2007, *J. Phy. Chem. Ref. Data*, 36, 1287